ABSTRACT

This project was on the suspension of fine particles in a fully-baffled flat-based cylindrical stirred tank of 155mm diameter using novel impeller designs by SATAKE Chemical Equipment MFG. LTD. as compared to a standard 4 pitched-blade impeller (4PBT) and 3-blade propellers (3P). The SATAKE impellers are an axial 3-blade HR100, a unique radial 4-blade HS604 and a large 2-blade MR203 impeller. The particles were (poly)methyl-methacrylate (PMMA) of diameters 18.6, 75.2 and 140.6 µm (SW, MW and LW, respectively) at concentrations 5, 10, 15, 20, 30 and 40% by weight, suspended in water filled to a height that gives 1:1 aspect ratio. Impeller clearance from the base were set at C/D=0.25, 0.50, 0.75 and 1.0, except for the HS604 and MR203 which were used only at an especially low clearance of C/T=0.02.

Increasing the clearance led to increased N_{js} and ε_{js} for all cases with very few exceptions between C/D=0.25 and 0.5 with the 4PBT. The HR100 and 3P of smaller diameter (d60) were the least affected by the clearance. The effect of clearance was also least significant with the MW particles; and suspending the SW particles required higher speed and energy with all impellers. Increasing particle concentration also led to higher speed and energy to achieve suspension, but again the HR100, HS604 and 3P (d60) were the least affected by the concentration change. These impellers were also the most efficient in terms of power requirement for just-suspension. The MR203 was the least efficient among all impellers, but its geometry is also very different and not designed for solid suspension.

The flow pattern generated from the impeller geometry directly affects the distribution of solids on the base, which in turn determine the speed and energy required to achieve suspension. S values obtained from Zwietering's equation show the strong

effect of clearance, particle size and concentration in the cases studied, which implies that the accuracy of prediction with Zwietering equation can be much affected by differences in any of the operating parameters.

ABSTRAK

Projek ini menkaji pergerakan butiran halus di dalam sebuah tangki silinder berukuran 155mm diameter. Tangki ini mempunyai empat sesekat yang ditetapkan pada 90^{o} dari satu sama lain. Prestasi pendesak rekaan baru dari SATAKE Chemical Equipment MFG. LTD. dibandingkan dengan pendesak biasa yang terdapat di pasaran iaitu 4PBT dan 3P. Pendesak SATAKE yang digunakan dalam kaijan ini ialah HR100, HS604 dan MR203. Pepejal yang digunakan ialah (poly)methyl-methacrylate (PMMA) yang bersaiz 18.6, 75.2 dan 140.6 μm (diwakili dengan symbol SW, MW dan LW) pada kepekatan 5, 10, 15, 20, 30 dan 40% berasaskan jisim. Tangki diisikan dengan air sehingga nisbah 1:1 ketinggaan. Jarak pendesak dengan tapak tangki ditetapkan pada 0.25*D*, 0.50*D*, 0.75*D* dan 1.00*D*, kecuali pendesak MR203 dan HS604, jarak ini ditetapkan sebagai 0.02T sahaja.

Semakin tinggi jarak pendesak dari tapak tangki (*C*), semakin tinggi N_{js} dan ε_{js} untuk semua eksperimen dalaml kajian ini, kecuali untuk pendesak 4PBT, N_{js} dan ε_{js} berkurangan apabila 4PBT digunakan pada C/D=0.25 dan 0.50. Prestasi pendesak 3P (d60) dan HR100 kurang dipengaruhi bila *C* ditukar. Kajian ini juga mendapati bahawa *C* kurang memberi impak kepada MW; tetapi kesan menukar posisi *C* adalah paling terserlah apabila SW digunakan di mana N_{js} dan ε_{js} adalah tinggi. Kepekatan serbuk pepejal yang digunakan juga menyumbang kepada N_{js} dan ε_{js} yang lebih tinggi. Namun, HR100, HS604 dan 3P (d60) juga merupakan pendesak di mana N_{js} dan ε_{js} kurang dipengaruhi. Pendesak-pendesak ini merupakan antaranya yang paling efisyen dalam penggunaan kuasa untuk operasi gaul-campur serbuk pepejal dan cecair. MR203 merupakan MR203 didapati merupakan pendesak yang kurang efisyen , tetapi rekabentuk yang unik ini adalah amat berbeza dengan pendesak yang lain.

Pengedaran aliran yang dijanakan dari pendesak akan mempengaruhi distribusi serbuk pepejal di tapak tangki. Kedua-dua parameter ini memutuskan kuasa yang diperlukan untuk serbuk pepejal dialihkan dari tapak tangki. Nilai *S* didapati dari persamaan Zwietering menunjukkan *C*, saiz dan kepekatan serbuk pepejal mempunyai pengaruh yang kuat ke atas nilai-nilai *S*. Ini bermaksud ketepatan persamaan Zwietering untuk meramal N_{js} akan dijejaskan oleh pelbagai parameter semasa operasi.

ACKNOWLEDGEMENTS

I would express my gratitude to Prof. Dr. Shaliza Ibrahim for always being generous to share her knowledge and experience. Her guidance and valuable advice led me to a smooth journey along this rocky path.

This research was financially supported by SATAKE Chemical Equipment MFG. LTD.

I would also like to acknowledge Mdm. Kalai Selvi, the lab technician, for providing helpful suggestions when experimental works do not go as planned. Not to forget, I would like to thank my friend, Inas F. Baker, and Zauyah Zamzam from SATAKE Chemical Equipment MFG. LTD., for their assistance in guidance for the experiments.

Last but not least, to my dearest family members. Thank you for being there to witness my falls, and always help me to get back on my feet again.

TABLE OF CONTENTS

LIST OF FIGURES

LIST OF TABLES

LIST OF SYMBOLS AND ABBREVIATIONS

Notations	Description	Units
Greek letters		
ε_{js}	Specific energy	Watt·kg^{-1}
μ_{SW}	Means for particles size 18.6 µm	
μ_{MW}	Means for particles size 75.2 µm	
μ_{LW}	Means for particles size 140.6 µm	
μ_{025}	Means for clearance 0.25	
μ_{050}	Means for clearance 0.50	
μ_{075}	Means for clearance 0.75	
μ_{100}	Means for clearance 1.00	
ρ_{SL}	Slurry density	kg·m^{-3}
ρ_{S}	Solids density	kg·m^{-3}
ρ_{L}	Liquid density	kg·m^{-3}
Roman Characters		
b_w	baffle width	mm
C	Clearance	mm
C_w	Solids concentration	wt%
D	Impeller diameter	mm
d_p	Particle size	µm
H	Mixing height	mm
H_0	Null hypothesis	
H_A	Alternative hypothesis	
m	Mass	kg
m_s	Mass of solid particles	kg
N_{js}	Just-suspension speed	rpm
p	Probability	
P_{js}	Power at just suspension	Watt
P/m_s	Power per unit mass of solids	Watt·kg^{-1}
S	Zwietering S value in N_{js} correlation	-
T	Tank diameter	mm

Notations	Description
Abbreviations	
3P (d60)	3 bladed propeller (60mm)
3P (d80)	3 bladed propeller (80mm)
4PBT	4 bladed 45^{o}Pitched-blade turbine (80mm)
BLGB	Blue lead glass ballotini
CBS	Complete off bottom suspension
ECT	Electrical capacitance tomography
ERT	Electrical resistance tomography
LDA	Laser Doppler anemometry
LED	Light emitting diode
LG	Large glass beads
LW	(poly)methyl metha-acrylate, 140.6 μm
MRI	Magnetic resonance imaging
MW	(poly)methyl metha-acrylate, 75.2 μm
PBT	Pitched-blade turbine
PIV	Particle imaging velocimetry
PMMA	(poly)methyl metha-acrylate
PTV	Particle tracking velocimetry
SATAKE	SATAKE Chemical Equipment MFG. LTD
SG	Small glass beads
SW	(poly)methyl metha-acrylate, 18.6 μm

LIST OF APPENDIX

CHAPTER 1

INTRODUCTION

1.1 Introduction

Solid-liquid mixing is found in many industrial processes as a means to achieve homogeneity or to improve mass transfer for a given chemical reaction, as in polymerization and heterogeneous catalytic processes. Reactors can come in various configurations, but the stirred vessel is widely encountered in the industries due to its simplicity and versatility. The mechanical agitation feature of the stirred tank configuration, however, means that much energy is drawn to drive the stirrer motor. Proper design and equipment selection are essential towards process optimization.

Solid suspension is the task of lifting solid particles and keeping them suspended in order to allow maximum contacting between the solids and liquid. This in turn facilitates any mass transfer between the two phases. Research studies are often conducted using model fluids and particles such as glass beads, metal beads, sand, and ion exchange resins. The work of Zwietering (1958) has become synonymous with the study of solids suspension in the stirred tank, as he pioneered the research using tanks, impellers, and particles of different sizes and concentrations to develop the widely cited empirical correlation to predict just-suspension speed (N_{js}); which is the minimum impeller speed to achieve suspension of all the particles. Beyond N_{js} it was determined that mass transfer is not significantly improved, as reported by Nienow and Miles (1978) in studying sodium chloride dissolution in stirred tanks. Zwietering's work has also been frequently referred to as it gives simple criteria for visually ascertaining "just-suspension".

Over the years, however, application of the correlation to studies of different impeller/tank configurations often showed that Zwietering's correlation has its limitations. Studies have been carried out using glass beads (Nienow, 1968; Ibrahim & Nienow, 1996), sand (Raghava Rao, Rewatkar & Joshi, 1988) or a bi-modal mix of different particles in the slurry (Baldi, Conti & Alaria, 1978; Ayranci & Kresta, 2011; Ayranci, Ng, Etchells & Kresta, 2013). Ibrahim and Nienow (1996) and Ayranci and Kresta (2011) studied the effect of varying parameters on the values of *S*, the geometric factor that accounts for geometric variations in Zwietering's correlation). The unconventional use of tank is recommended for mineral processes of high concentration (Wang, Boger & Wu, 2012); while low energy suspension with conventional impellers have been found to be feasible for shear-sensitive systems such as in mammalian cell culture (Ibrahim & Nienow, 2004). Traditional impeller designs that have been studied are marine propellers, pitched-blade or mixed flow turbine, and the classic Rushton disc-turbine. Improved patented designs that have been reported are impellers such as the Intermigs, A310, HE-3, and the curved-blade types.

The anticipated outcome of this work is to be able to gain further insight into the solid-liquid suspension behaviour in a stirred tank, and the parameters that affect suspension efficiency. This study aims to increase the understanding of solid suspension in stirred vessel using impeller designs which have not been published before, namely the HR100, HS604 and MR203 by SATAKE Chemical Equipment MFG. LTD. These impeller geometries are quite different from what have been reported in the literature, and it is of interest to see how they fare in terms of solid suspension compared to the more traditional geometries in suspending fine, lightweight solid particles in a stirred tank. The polymer particles, at high concentrations and very small size range have not been reported in the literature either.

1.2 Objectives

This study is on the suspension of solid particles in liquid using the stirred vessel with a select range of impeller/tank configuration, solid concentration and rotational speed. The objectives are to investigate:-

(1) how the suspension behavior is affected by variations in the parameters

(2) the relative performance of various geometries under different conditions

(3) is Zwietering's correlation suitable for the whole range of conditions studied

The suspension behavior is observed mainly on the tank base, but is very much dependent on the flow patterns created by the impeller/tank geometry, rotational speed and solid concentration. Impeller efficiencies are determined by the power input to achieve just-suspension, and how much affected is the impeller by changes in the system conditions. Finally, substituting the data in Zwietering's equation enables the calculation of the *S* value, and an analysis of this will show the range within which the correlation can fairly well predict the just-suspension.

1.3 Outline

Chapter 1: Introduction

This is an introductory chapter to the research, its objective and an outline of the report layout.

Chapter 2: Literature Review

This chapter presents some fundamental of solid-liquid mixing and the parameters that affect the energy efficiency in solid-liquid mixing.

Chapter 3: Methodology

Description of the approaches to achieve research objective is reported in this chapter. Detailed description of the experimental setup, impeller design, materials and experimental procedures is presented.

Chapter 4: Results and Discussion

This chapter reports the findings from the experimental studies to compare the performance of conventional impellers and novel design impellers. The power consumption at the particles' just-suspension speed of the impellers is used to compare the impeller performance.

Chapter 5: Conclusion and Recommendation

Summary of findings from the experimental results in this study is presented. Recommendations for future research are also included.

CHAPTER 2

LITERATURE REVIEW

2.1 Introduction

In 1989, poor mixing was known to result in an estimated loss of $1billion to $10 billion in the United States of America chemical industry. In a multinational chemical company, the loss in year 1993 itself was up to $100 billion (Paul, Atiemo-Obeng, & Kresta, 2004). This information highlights the high process cost due to poor mixing. Expenses of the mixing process could also be cut down from other means. As the energy saving design for processes are globally practiced, attention should also be given to applying energy saving in mixing processes. Over mixing is inefficient, and may cause segregation of the mix (Ayranci & Kresta, 2011). The poorly mixed slurry is no longer suitable for its original purpose and has to be discarded. All these are losses incurred in the production process.

Solid-liquid contacting is important in the processing industry, ranging from catalytic reaction systems to polymerization, and from fermentation processes to sludge treatment and ore processing. Studies on solid-liquid mixing in stirred tank have used a variety of solid particles, usually based on their ease of availability. The most common are sand in water (Zwietering, 1958), glass beads (Zwietering, 1958; Nienow, 1968; Raghava Rao et al., 1988; Ibrahim & Nienow, 1996; Wang, Boger & Wu, 2012; Wang, 2010; Wu, Zhu, Bandopadhayay, Pullum & Shepherd, 2000; Wu, Zhu & Pullum, 2002), bronze particles (Machado, Nunhez, Nobes & Kresta, 2011), and ion exchange resin (Ayranci & Kresta, 2011). Studies have also been reported with lead shots (Ibrahim & Nienow, 1996) and Cytodex microcarrier particles to illustrate very light, neutrally buoyant particles (Ibrahim & Nienow, 2004). Wu et al. (2000), Wu et al. (2002) and Wang et al. (2012) have reported several works with heavy particles and very high concentrations to represent conditions in minerals processing, but in general studies using liquids and particles actually used in industrial applications are still uncommon. Water is most commonly employed as liquid phase; while corn syrup solutions and other more viscous fluids have also been studied.

There have been no standard or design rules for solid liquid mixing in stirred tank, other than the recognition that complete off-bottom suspension is important for maximum contact between the particles and liquid. Studies have been carried out to compare the mass transfer with homogeneous and non-homogeneous dispersion and it is reported that the mass transfer increases significantly when the particles are fully (just) suspended (Nienow, 1992), but no significant increase in mass transfer happens when particles are homogeneously dispersed (Nienow & Miles, 1977). Once they are just suspended, although significantly high energy is required to go from just-suspension to homogeneous suspension. Since then, studies on solids suspension have focused mainly on the point of just-suspension; and this has raised questions such as, how to define and determine the minimum impeller speed for just-suspension (N_{js}), and what are the influencing factors.

2.2 Determination of just-suspension speed

Optimization of the solid liquid mixing in stirred tank is often associated with the just suspension speed. A definition for the point when the solids achieve the "just-suspension" state is needed. Over the years, a number of methods have been developed with respective justification. However the method definition often depends on the objective of the research.

From the point where the total surface area of solid particles has complete contact with liquid, the increase of mass transfer from solid particle to the liquid is only minimal (Paul et al., 2004). Zwietering (1958) defined N_{js} as the point when no solid particles remain at the tank bottom for more than 1-2s, or it is more commonly referred as the complete off-bottom suspension (CBS) criterion. This assumes that as long as the particles are moving they are deemed suspended or lifted from the tank base, determining this point is by visual observation and thus very subjective. Some researchers may allow a reproducibility of up to 5% (Nienow, 1968; Armenante & Nagamine, 1997) and as some go for as low as 1% (Wu & Pullum, 2002).

Regions of stagnation may be present where particles require impeller speed of 20-50% higher to be completely lifted (Kasat & Pandit, 2005). It is inefficient to increase the impeller speed to such great extent to lift a relatively small percentage of particles that remained at tank bottom. Chudacek (1985) applied a modification in the CBS criterion where the last amount of solids that require excessive power input to be suspended is not taken into the suspension criterion. Sharma and Shaikh (2003) used a similar criterion in their study where the unsuspended solids in the fillet corners of the tank are excluded from the suspension criterion. Hicks, Meyers and Bakker (1997) suggested that N/N_{js} is 80% when about 10% of the solids is not suspended (periodically moving but not suspended). Since this method has only been developed in recent years, only several studies on solids suspension referring to this method are available.

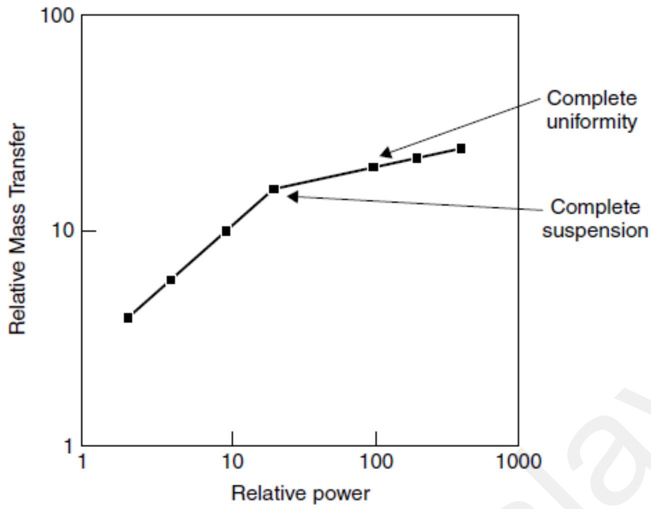

Figure 2.1: Effect of relative impeller power on relative mass transfer (Paul et al., 2004)

2.2.1 Visual method

The solids distribution at tank bottom is observed from an inclined mirror placed below the tank bottom. This method of determining the CBS condition highly depends on the worker's observation and the reproducibility of the results with this method is important. In order to overcome the limitations of this method, Baldi et al. (1978) had several workers to examine the suspension states in their study and the agreed N_{js} is confined within 10% of the average values. It can be difficult to determine the N_{js} of particles in the solid liquid mixing in slurries of high concentrations or dark particles. When observations are made with the naked eye, adding dye into the liquid (Wang, 2010) and/or using tracer particles of similar density and size with the particles used in experiments, as contrast in color could be helpful to assist in the visual observations. Fine powders may come off from some particles i.e. palm shell activated carbon, and the fine particles could disturb the observation (Ibrahim, Jasnin, Wong & Baker, 2012).

2.2.2 Non visual method

Advanced technology are available to overcome the limitation of visual observation, though these tools can be costly. Tomography is a recent tool used to investigate the flow pattern, which earlier are determined using particle imaging velocimetry (PIV) or laser Doppler anemometer (LDA) (Kumaresan & Joshi, 2006). The N_{js} is also determined using other non-intrusive methods, e.g. electrical resistance tomography (ERT) and electrical capacitance tomography (ECT). Tomography does provide promising information of the flow in mixing system (Mavros, 2001). However, conductive material (e.g. organic fluids, metal impeller) is not suitable to be used in an ECT (Paul et al., 2004).

These instruments are helpful to have experiments conducted in the region almost impossible for the human eye, e.g. in high concentration (>30%) slurry. Not just the flow at the tank bottom, the cross-sectional flow from the sides can be plotted with the help of electrical tomography. Hosseini, Patel, and Mozaffari, (2010) successfully determined the flow of a solid-liquid system in agitated tanks, up to 30% by weight, using an electrical resistance tomography. In solid-liquid mixing studies, it is suggested to digitally remove large solids from the image in post-processing to apply of PIV for solids up to 1.5% concentration (Virdung & Rasmuson, 2007). Stevenson et al. (2010) compared magnetic resonance imaging (MRI) and ERT in solids suspension studies. The authors suggest MRI provides better spatial resolution and more detail compared with qualitative optical observations; the ERT is for much faster temporal resolutions and large length-scales.

2.3 Correlations for the just-suspension speed (N_{js})

Over the years, several correlations to predict the N_{js} have been established. The Zwietering correlation is the most commonly cited equation for N_{js} prediction. Zwietering (1958) carried out a range of experiments varying the particle concentration (X), particle and fluid density (ρ_L and ρ_s), particle diameter (d_p), impeller diameter (D) and viscosity (ν) to obtain the empirical relationship of Equation (1).

Table 2.1: N_{js} Correlations

Equation	Reference	N_{js} Correlation	Remarks
(1)	Zwietering, (1958)	$N_{js} = \frac{S\upsilon^{0.1} d_p^{0.2} (g\Delta\rho/\rho_L)^{0.45} X^{0.13}}{D^{0.85}}$	Unimodal slurry up to 20wt% 2 tank sizes Flat bottom tank
(2)	Nienow (1968)	$N_{js} \propto \frac{d_p^{0.21} (g\Delta\rho/\rho_L)^{0.43} X^{0.12}}{D^{2.21}}$	unimodal slurries with 0.5g solids Disc-turbine Flat bottom tank
(3)	Baldi et al., (1978)	$N_{js} \propto \left(\frac{g(\rho_L - \rho_S)}{\rho_L}\right)^{0.42} \frac{\upsilon^{0.17} d_p^{0.14} X^{-0.125}}{D^{0.89}}$	Unimodal and bi-modal slurries up to 20wt% Disc-turbine Flat bottom tank
(4)	Raghava Rao et al., (1988)	$N_{js} = \frac{S\upsilon^{0.1} d_p^{0.11} (g\Delta\rho/\rho_L)^{0.45} X^{0.1}}{D^{0.85}}$	Unimodal slurry up to 50wt% 5 tank sizes Flat bottom tank
(5)	Ayranci et al., (2013)	$N_{js} = \left(\frac{\rho_{sl.1} N_{js.1}^3 + \rho_{sl.2} N_{js.2}^3}{\rho_{SL,mix}}\right)^{1/3}$	Bi-modal up to 27wt% PBT and A310 impellers Flat bottom tank

Zwietering's (1958) work was still limited to only two tank sizes and unimodal slurry with solids concentration up to 20wt%. Raghava Rao et al. (1988) conducted a study up to 50wt% of solids concentration with five tank sizes.

As research scope expanded over the years to cater to needs in industrial applications, Machado et al. (2011) suggested that Equation (1) should be applied only to estimate solids of concentration less than 10% by weight. Stevenson et al. (2010) examined the particles distribution of 5-10% using ERT and MRI. The authors reported that Equation (1) over-predicts the critical impeller speed, as adequate particle suspension was achieved below the predicted N_{js}.

Despite the limitations present in Equation (1), it is still commonly used to predict N_{js}. Ayranci et al. (2013) recommends the use of experimental N_{js} for unimodal slurry. Baldi et al. (1978) studied on solids suspension with mixed solids. Suspension of the mixed solids is studied and another correlation is proposed, as shown in Equation (3). This study only covered a range of low concentrations where particle-particle interactions have not caused significant impact to the system. Ayranci et al. (2013) then studied mixed solids system up to 27wt%.

The geometric factor S was introduced in the Equation (1) by Zwietering (1958) and the author reported the effect of impeller diameter on the S values. For all studied impellers the S value increases with increasing T/D ratio, except the propeller. At D/T>0.45, a change in flow pattern was found at the tank base and at the same point, the S values decreases at increasing T/D ratio. A similar trend was also observed with a range of HE-3 impeller diameters (Ibrahim & Nienow, 1996). Ayranci and Kresta (2011) studied on the effect of clearance on S values, and suggested that the effect of off-bottom clearance on S values is small for C/T<0.25 but shows a significant increase when a secondary circulation loop is present. Increase in fluid viscosity changes the S values up to 90% (Ibrahim & Nienow, 1999). Work with activated carbon as particles (Ibrahim et al., 2012) have shown that in addition to the particle properties size, density and concentration S is also a function of porosity.

2.4 Impeller geometry

The impeller and shaft, being the part that is in contact with both the motor and the mixture, is the means by which electrical energy that has been converted into mechanical energy by the motor and transferred into the mixture to create the mixing energy. The shaft transports the energy from the motor and dissipates it via the impeller when it comes in contact with the mix in a rotational motion. The selection of the right impeller geometry for a designated mixing operation is crucial in order to have the mixing process conducted efficiently.

Generally, impellers are grouped into two, the axial impellers that produce good bulk flow and radial impellers that are known for high shearing, the most commonly used being the Rushton disk turbine. Impellers are compared based on their power number, N_P. The power number is the most important characteristic of an impeller (Machado et al., 2011) with high values (N_P>3) for radial impellers due to their shearing action, and low power number (N_P=0.1-0.5) for the low shear, high flow axial impellers. The dimensionless power number is a measure of relative power consumption.

$$N_P = \frac{P}{N^3 D^5 \rho_{SL}} \qquad \text{-Equation (6)}$$

where P is the power required by the impeller to produce the desired mixing task and P is based on measurement other than electrical input. P is also the power imparted into the vessel content. The denominator is a combination of the impeller speed, N, impeller diameter, D and fluid density, ρ_{SL} all of which are parameters that influence the energy of the mixing operation.

2.5 Effect of impeller geometries on power consumption

Bates, Fondy, and Corpstein (1963) studied the effect of impeller geometries on impeller power number for a range of Reynolds number including laminar, transitional and turbulent flow. Impellers with different number of blades, blade geometry, blade angle and with or without disc, are conducted

Disk flat-blade impellers (Rushton) are found to have higher power requirement as compared flat-blade impeller without disk. Ibrahim and Nienow (1999) worked on solids suspension in the transitional regime. Their results also meets agreement with this as it suggests the efficiency of the Rushton is the lowest as compared to other impellers (Chemineer HE-3, Ekato Intermig, downward pumping, and Lightnin' A310) used in this study.

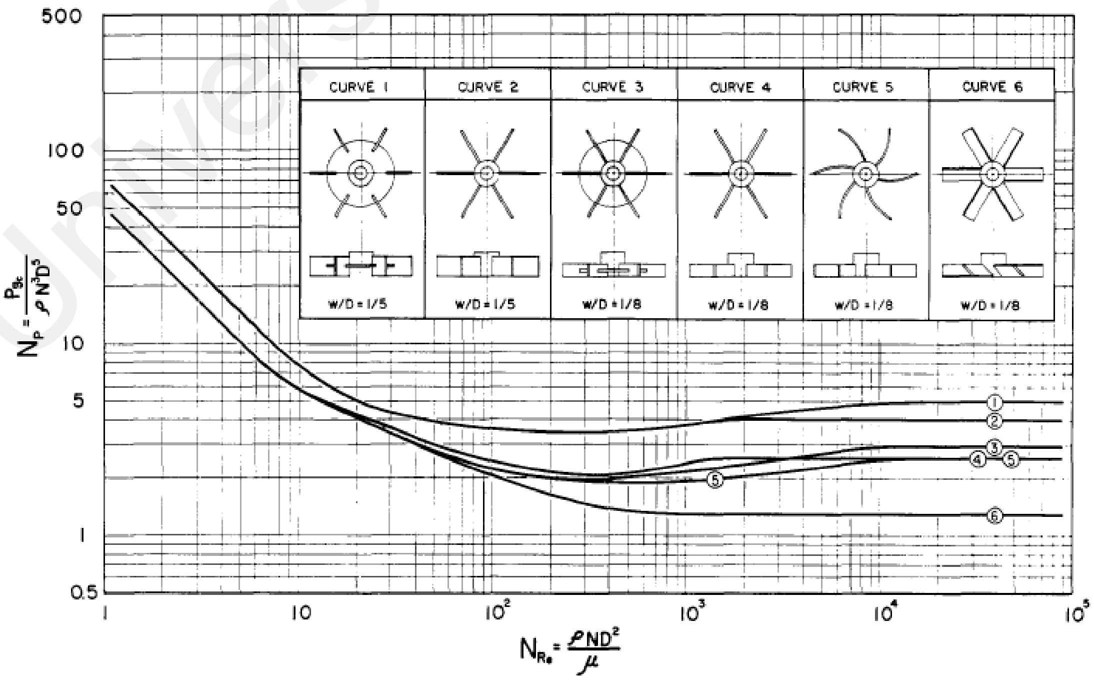

Figure 2.2: Power number-Reynolds number correlation fluids for various turbine impeller designs (Bates et al., 1963)

The flow quality is highly dependent on the impeller design. Kumaresan and Joshi (2006) reported the flow pattern of different impeller geometries by varying the impeller design, impeller diameter, number of blades, blade angle, blade width, blade twist, and pumping direction. In solids suspension, a *T*/3 impeller is more efficient compared to a *T*/2 impeller, as less energy loss (Ayranci et al., 2012). The number of blades gives little effect to the power number, however the pitch angle for pitch blade impellers has minimum effect on the efficiency for particle suspension (Jirout & Rieger, 2011). Properties of the particles have to be taken into account during impeller selection. An up-pumping pitched blade impeller is recommended when suspending floating particles, however the mixing time increases with increasing particle size and bulk concentration (Kuzmanić & Ljubičić, 2001).

The flow pattern induced in a vessel changes with the impeller geometry, tank geometry and impeller/vessel configuration. Nienow and Miles (1978) observed the flow pattern of pitched-blade turbines and concluded that such impellers are very sensitive to impeller size and clearance. The point of last suspension also changes with different impeller geometries. Raghava Rao et al. (1988) reported that particles at the annular space around the centre are last to suspend for disk turbine and upward pumping pitched-blade turbine; and for the downward pumping pitched blade impeller, particles at the periphery are last to be suspended. Ibrahim and Nienow (1995) used halogen lamp to illuminating tracer particles and determine the flow patterns by observing the streak lines. The change in the flow pattern by adjusting the clearance and viscosity was shown. At constant power input, the change in impeller blade pitch-angles and number of blades produces similar velocities in the turbulent regime, but energy efficiency is improved in low Reynolds number (Wu, Graham, Nguyen & Mehidi, 2006). Aubin, Le Sauze, Bertrand, Fletcher and Xuereb (2004) plotted the flow pattern in an aerated stirred tank with particle imaging velocimetry (PIV) and the radial velocity profiles were reported. Flow pattern with and without the presence of gas phase were presented and introducing gas phase in a stirred tank system changes the flow pattern.

Wang et al. (2012) worked with ultrahigh concentration slurries and pointed out Raghava Rao et al. (1988) and Ibrahim and Nienow (1999)'s studies covers only relatively lower concentration slurry. Wang et al. (2012) reports that at slurry of high solids concentration, the axial impellers still perform better, under baffled condition however when baffles are removed, the radial impeller (Rushton turbine) could perform better than the axial impellers.

2.6 Effect of particles properties on power consumption

Particle properties including the size, density, hardness would need different configuration to achieve suspension efficiently. Glass beads or sand ($\rho_s \approx 2500 kgm^{-3}$) of different sizes are often used as the solid phase in solids suspension studies (Zwietering, 1958; Wang et al., 2012).

Raghava Rao et al. (1988) expanded the scope by using glass beads of wide range of sizes and calculated the terminal settling velocity of the particles in the water. He explains that large particles has higher power requirement are heavier and settles faster (Table 2.2). This increases energy requirement to suspend the settling particles.

Wang et al. (2012) studied on solids concentration up to 125% by weight has similar findings with Raghava Rao et al. (1988). As particles of smaller sizes requires less power to be lifted. Wang et al. (2012) suggests that for a same concentration of solid particles, breaking particle sizes down to smaller size will optimize mineral intensification process.

To suspend increased particle sizes, a higher N_{js} and torque is needed (Raghava Rao et al., 1988).Wang (2010) studied the effect of solids concentrations with glass beads at high concentration. ε_{js} showed a steep increment at the larger particle size range but ε_{js} appears to be similar for particles of the lower sizes.

Table 2.2: Particle size and terminal velocity

Reference	Particle type	Particle density (kgm^{-3})	Solid size (μm)	Terminal velocity in water (mm/s)
Raghava Rao *et. al.*, 1988.	Quartz (granular)	2520	• 100 • 340 • 700 • 850 • 2000	• 34 • 76 • 104 • 134 • 165
Wang et al, 2012.	Glass beads (sphere)	2500	• 70-100 • 110-235 • 260-480	• 9.4 • 14.2 • 46.0

Particles of density similar to water can be suspended with slight agitation, when mixing time is not a limiting factor (Ibrahim & Nienow, 2004). Particles with elastic properties, such as ion exchange resin and PVC discs, are able to dissipate energy in the form of heat and absorb energy; hence more energy is needed to suspend the particles, especially in higher concentrations (Bubbico et al., 1998). Momentum transfer in the form of particle-particle collision has significant effect for solids suspension, the momentum occurs between hard particles (glass beads and nickel) appears to be more significant than collision between ion exchange resin and glass beads (Ayranci & Kresta, 2011).

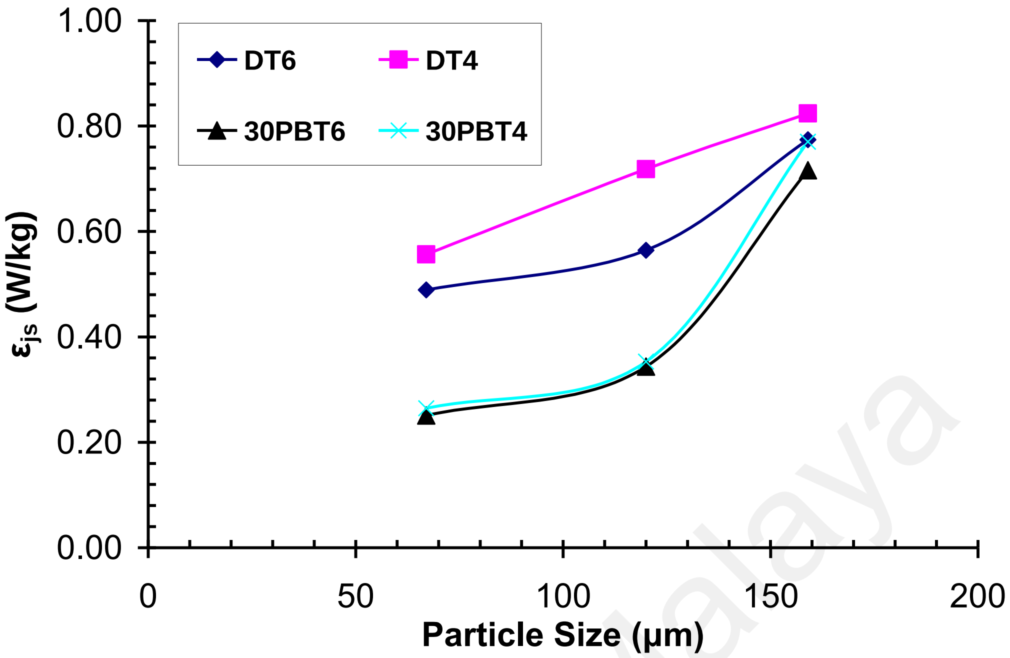

Figure 2.3 Effect of particle size on ε_{js} for Rushton disk turbines and pitch-bladed impellers at C_v = 0.4 v/v. Tank configured in the baffled condition. (Wang, 2010)

Small-sized particles and light particles are suspended with very low mean specific energy dissipation rate (Bujalski et al., 1999). Larger-sized particles would require more energy lift the particles as the settling velocity increases. Large particle size and high solids loading results in lower axial concentration distribution, as the solids loading contributes to higher pressure during solids suspension (Ochieng & Lewis, 2006). In ultra-high solids concentration (50vol% or 125wt%), it appears at lower d_p, similar amount of energy is required to suspend particles at ≈70 μm and ≈120 μm (Wang et al., 2012). Introducing a second solid phase in the system would significantly affect the mixing, especially in mixture above 20wt% solids as the particle-particle interactions becomes significant (Ayranci & Kresta, 2012).

2.7 Effect of solids concentration on power consumption

Bubbico et al. (1998) worked with large particles (>1mm) and finds that dispersion power increases with solid concentration. Similar to findings by Raghava Rao et al. (1988), Bubbico et al. (1998) explained that energy dissipation in solid collision and solid liquid friction may not be significant at low solids concentration. However, it will be appreciable as impact frequency between solid particles is higher at increasing solid concentration. Particle-particle interactions were found to dominate power requirement when the concentration is higher than 25% (Ayranci & Kresta, 2011).

Wu et al. (2002) reported that radial impellers (Rushton) are more energy efficient than axial impellers (pitched blade) at high solids concentration slurry when working with particles of smaller sizes (~100μm). At high solids concentration, the slurry may behave like Newtonian fluid and the rheology of the fluid changes. In studies of different concentrations range, the effect of concentration to the N_{js} may be very different. The generalized equation could also be different with the actual condition when dealing with high concentration mix.

Wang et al. (2012) and Wang (2010) suggested that a critical concentration where the minimum specific power is present. The specific power decreases with increasing solids concentration up to the critical concentration, and the specific power increases with increasing concentration. The critical concentration where minimum specific power is designated as the optimum solids concentration.

Table 2.3: *a*-Exponent for Zwietering Correlation (N_{js} α X^a)

Reference	Solids concentration	*a*-Exponent
Zwietering, 1958	0.5-20	0.13
Raghava Rao et al., 1988	0-50	0.1
Wu et al., 2002	40-50 vol% 100-125wt%	0.60-0.80 (Axial) 0.30-0.40 (Radial)

2.8 Effect of off-bottom clearance on power consumption

Impeller off-bottom clearance is defined as the distance from tank base to the centre of the impeller hub, unless stated otherwise (Ayranci & Kresta, 2011).

Zwitering (1958) is the first to identify the effect of off-bottom clearance on N_{js}, he suggests that the clearance could not be expressed in a power law form. Chudacek (1986) also agrees that using power law form gives poor correlation with the clearance effect.

Nienow (1968) explains that flow pattern varies at high and low clearances for impellers, and solids distributions are affected by the two different flow patterns. Nienow and Miles (1977) later reported that at low off-bottom clearance and small D/T, the 45º pitched blade turbine has better energy efficiency in particle-mass transfer. In solids suspension at very low clearance system Armenante and Nagamine (1997) suggested that both axial-flow and mixed-flow impellers are more energy efficient to suspend particles as compared to radial-flow impellers.

At close to the base the impeller, local energy to energy dissipated per unit volume is constant (Shaikh & Sharma, 2003). The work reported three regions of impeller clearances where the impeller flow behaves differently and affects the power for solids suspension. At the first region, where clearance is up to C/T=0.1, a single-eight flow pattern is generated. A second loop of flow is induced between the impeller and the tank base in the second region. Higher impeller rotational speed and power is required to free the particles trapped by the flow. Gray (1987) explains that an axial impeller could behave like a radial impeller at C/T>0.35. As the clearance gets higher, the secondary flow expands and forms a radial flow pattern, similar to the flow pattern of a Rushton turbine.

When it reaches the third region at C/T=0.35, the secondary flow further expands and the flow forces the particles towards centre (at the tank base). The steep hike in Figure 2.4 at the third region indicates the sudden increase of N_{js} and also P_{js} at C/T>0.35, as the axial impeller now behaves like a radial impeller

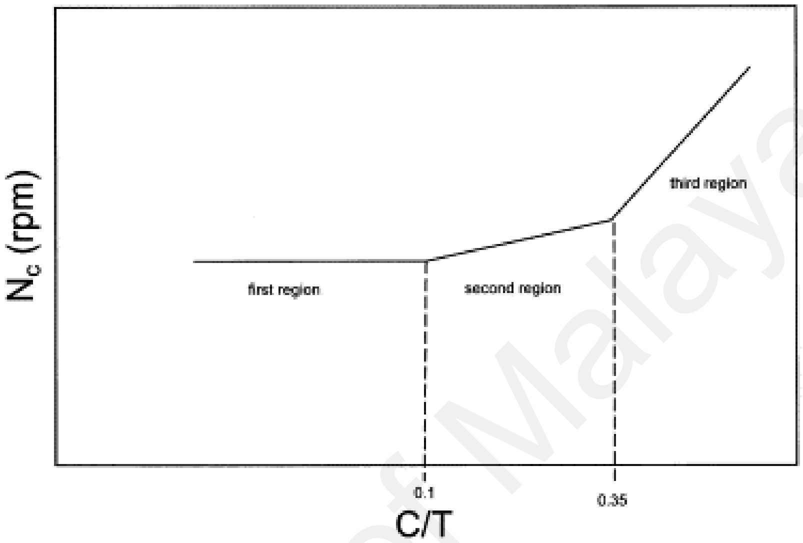

Figure 2.4: illustration of the effect of impeller clearance on critical impeller speed of suspension (Shaikh & Sharma, 2003)

The discharge flow for a PBT has a strong interaction with the tank walls, and power number can differ ~15% by changing the position of the impeller in the tank (Chapple et al., 2002). Jirout and Rieger (2011) reports that propellers are more sensitive to impeller clearance compared to hydrofoil impellers and pitched blade impellers; and Ayranci and Kresta (2011) reported in bimodal system, A310 impeller has lower P_{js} compared to a pitched blade impeller.

Based on current research trend in solid liquid mixing, studies covering lightweight fine particles of d_p<100micron is still not available. This work aims to fill this gap and investigate the suspension of such fine solids up to high concentrations. Innovative impeller designs from SATAKE are employed to observe how they perform in the fine particles system compared to conventional impellers.

CHAPTER 3

METHODOLOGY

3.1 Experimental Setup

A cylindrical, flat-based Perspex tank of internal diameter, T=155 mm was used in the experiments. The tank was fully baffled (b_w = 0.1T) and it was placed in a rectangular tank filled with water to enable visual observation of the cylindrical tank content without distortion. A mirror placed at a 30° angle below the tank facilitates visual observation of the tank base in ascertaining the state of particles suspension. In addition, visual observation was aided with the shine of a white LED lights and sun-shades to reduce reflection.

The stirred tank setup as illustrated in Figure 3 (a) is used for N_{js} determination. The impeller in use was mounted on a 10mm diameter shaft which was then connected to the SATAKE S3000 II torque transducer, as shown in Figure 3 (b). Impeller rotational speed is controlled with the torque transducer, and torque measurement is taken with a computer connected to the torque transducer using SATAKE StirPC (software).

The solid particles employed were (poly)methyl-methacrylate(PMMA) particles of density, ρ_s=1300 kgm^{-3} and particle diameters (d_p) 18.6 μm, 75.2 μm and 140.6 μm (hereinafter known as SW, MW and LW, respectively), while tap water (ρ_l=1000 kgm^{-3}) was used as the liquid phase. Table 3.1 gives the solid particles properties. The particles concentrations, C_w studied were 5wt%, 10wt%, 15wt%, 20wt%, 30wt% and 40wt%. The cylindrical tank was filled with the mixture of water and PMMA particles of a given concentration, to a height equal to the tank inner diameter, giving an aspect ratio of 1:1.

Terminal velocity of the solid particles are shown in Table 3.1. The terminal velocity is calculated using Equation (7):

$$V_t = \frac{g{d_p}^2(\rho_s - \rho_l)}{18\mu} \qquad \text{Equation (7)}$$

Where

V_t is the terminal velocity in m·s^{-1}

g is the gravitational acceleration in 9.81m·s^{-2}

d_p is the particle size in m

ρ_s is the solid particles density, 1300kg·m^{-3}

ρ_l is the water density in 1000kg·m^{-3}

µ is the dynamic viscosity of the liquid, 0.001kg/s·m

The just-suspension point was visually determined with the naked eye based on Zwietering's criterion of particles not remaining stationary at the bottom of the tank for more than 1-2s. It was not an easy task considering fine particles were used up to high concentrations. Regions of stagnation may be present where particles remained vibrating at their respective location even at very high impeller rotational speed. These stagnant particles were not taken into account for the Zwietering's criterion. Particles movements on the tank base were repeatedly and carefully observed before a value was decided for N_{js}. Due to the subjective nature of this method, a variation of ±5-10 rpm in N_{js} is considered acceptable. The determined N_{js} was examined again the next day before torque reading was taken.

Table 3.1: Solids properties

	d_p (µm)	ρ_s (kgm^{-3})	Terminal velocity (m/s)
SW	18.6	1300	5.66×10^{-5}
MW	75.2	1300	9.25×10^{-4}
LW	140.6	1300	3.23×10^{-3}

Table 3.2: Particles-water content at each C_w

Concentrations ratio (wt/wt)	Weight of the solid particles, (g)	Water volume (mL)	Weight of the water (g)	Apparent density (kgm^{-3})
0.05	147.942	2810.898	2810.898	1015
0.10	299.379	2694.409	2694.409	1030
0.15	454.435	2575.134	2575.134	1145
0.20	613.244	2452.974	2452.974	1060
0.30	942.672	2199.568	2199.568	1090
0.40	1288.851	1933.276	1933.276	1120

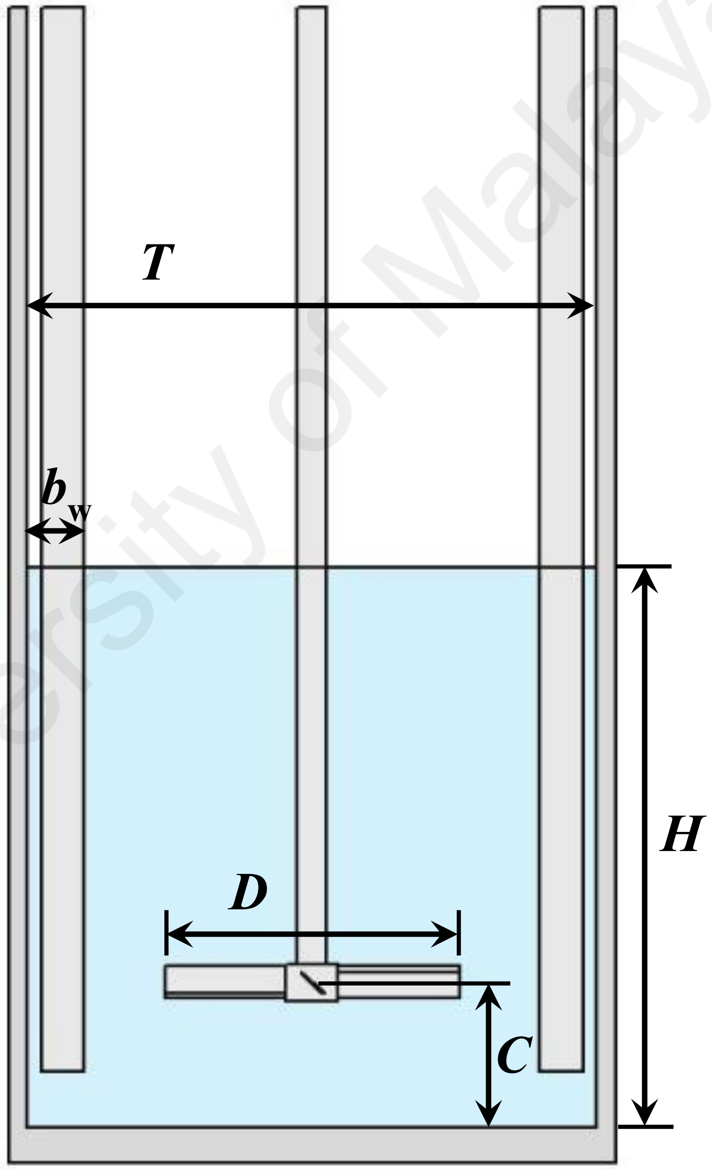

(a)

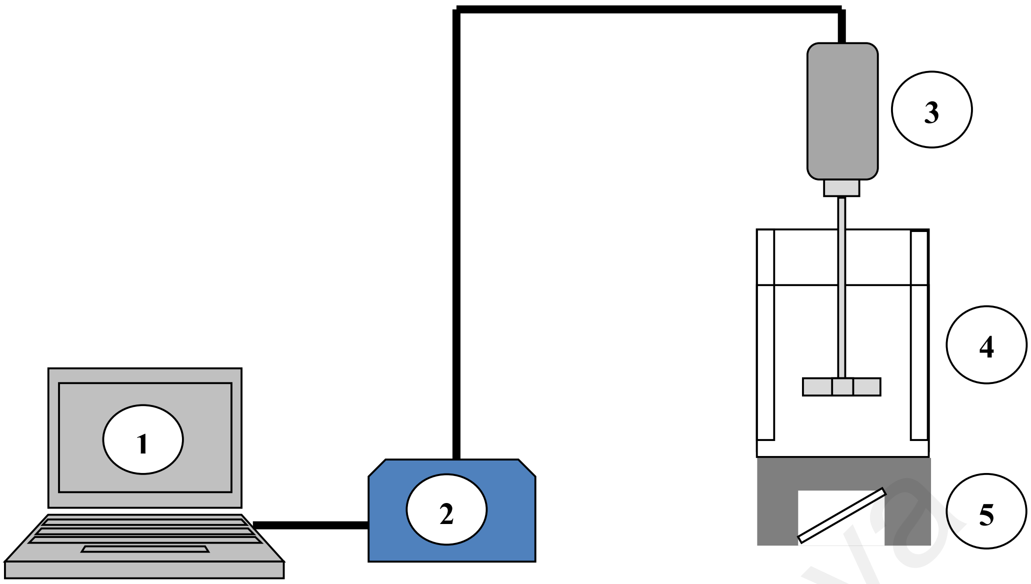

(b)

Figure 3.1 Experimental setup (a) Cross section of cylindrical tank (side view);(b) Experimental setup (1) Computer, (2) Torque transducer SATAKE® ST-3000II, (3) motor, (4) cylindrical tank, (5) stand with inclined mirror

3.2 Impeller geometries

Six impellers were studied in this work, a 4-pitched blade turbine with 45^o blade angle (4PBT), a 3-blade propeller of 80mm diameter (3P (d80)) and 60mm diameter (3P(d60)) and three novel designs, the axial impeller HR100, radial impeller HS604, and large impeller MR203 by SATAKE Chemical Equipment MFG. LTD. The impeller conceptual drawings and schematic diagrams are as shown in Figures 3.2-3.8, and the impeller specifications are given in Table 3.3.

HR100 is a low shear axial impeller with high discharge performance. It is suitable for liquid-liquid mixing in medium and high Reynolds number range, solid-liquid mixing and uniform suspension of fragile or lightweight particles and emulsified micro-capsules.

The unique 4-blade HS604 is mounted close to the base to create radial flow along the tank base and close-up to the tank wall in order to create large circulation, and extremely high discharge flow. Its flow characteristic ensures flow stability in the stirred tank even though liquid surface changes and it is suitable to use at very low liquid level. This enhances uniformity of solids distribution. Its unique profile of mounting method and relatively simple shape blade structure make this impeller ideal for pharmaceutical, biochemical and food industry processes and in reactive mixer where uniformity and liquid level changes is critical.

MR203 is a large, two-blade impeller. It has a serrated blade design, and trapezoidal blade shape with a wider dimension at the bottom to create flow towards the tank bottom. The full height of this impeller may exceed the liquid height, with the blades protruding the water surface; and the diameter covers ≈70% of the tank base area. Set at a low clearance of $0.02T$, the clearance effect at the axial centre generates a powerful suction flow, to create a large circulation flow.

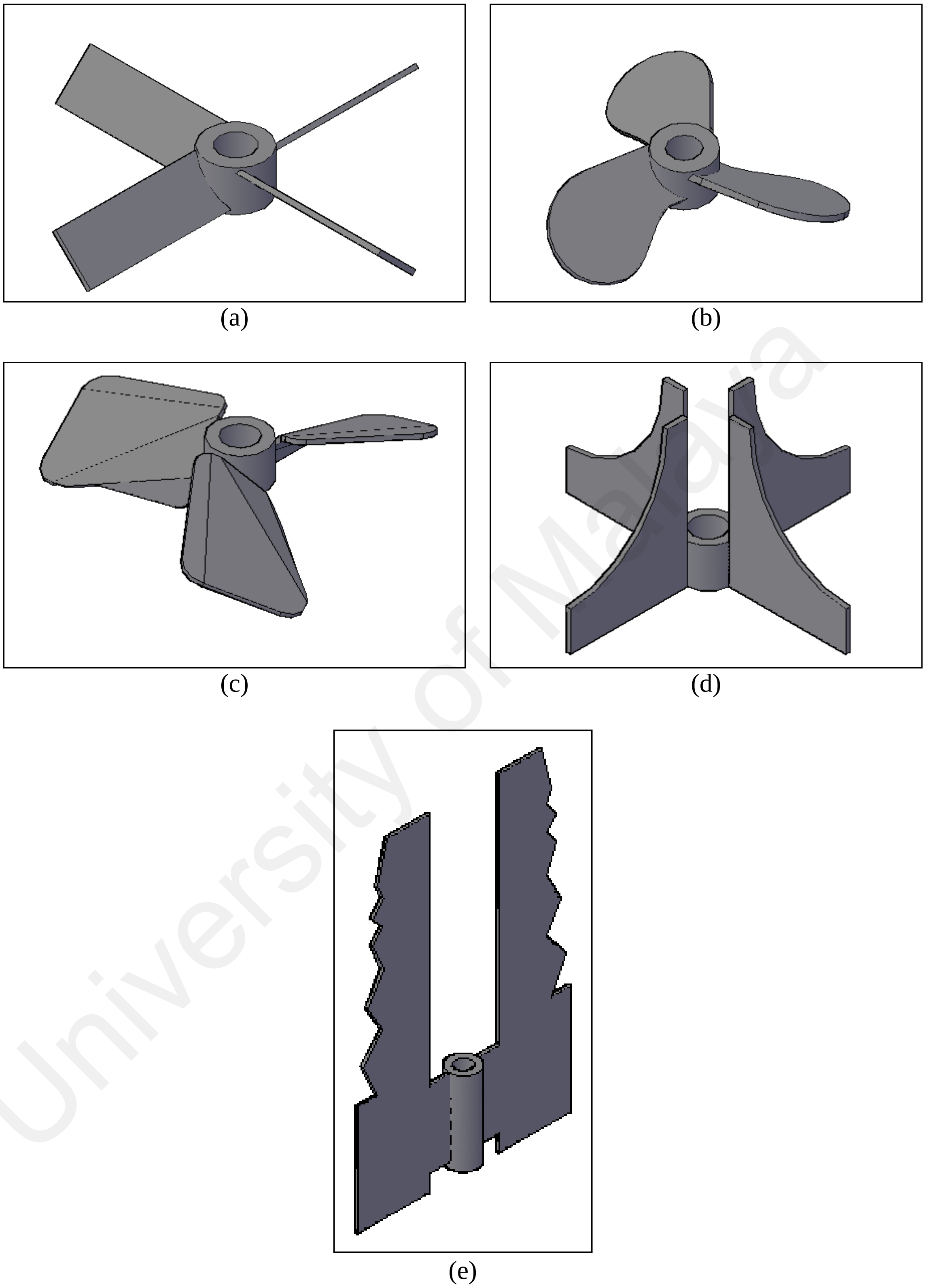

Figure 3.2: Conceptual drawings of impeller (a) 4PBT; (b) 3P; (c) HR100; (d) HS604; (e) MR203

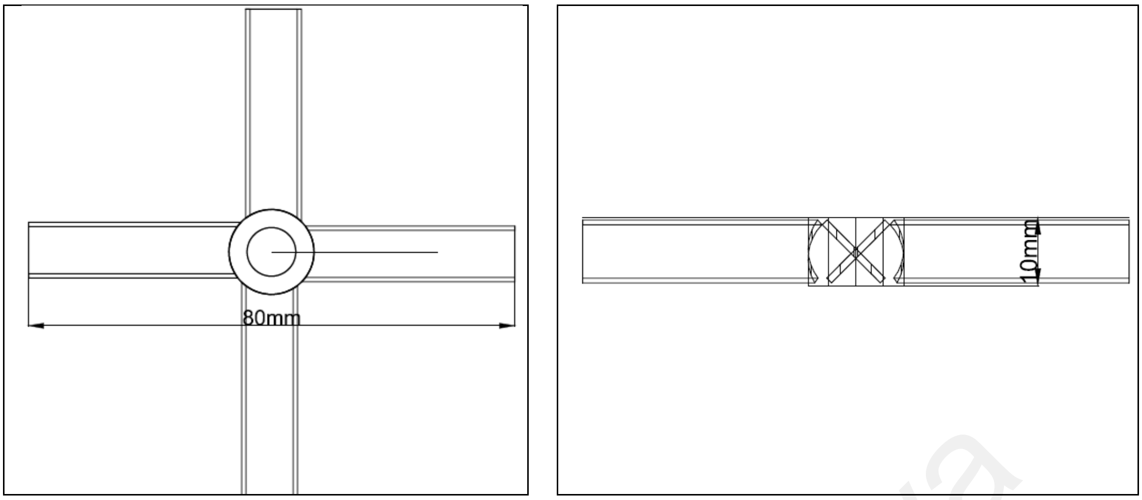

(a) (b)

Figure 3.3: Schematic diagram for 4PBT, 45° pitched blade
(a) top view; (b) side view

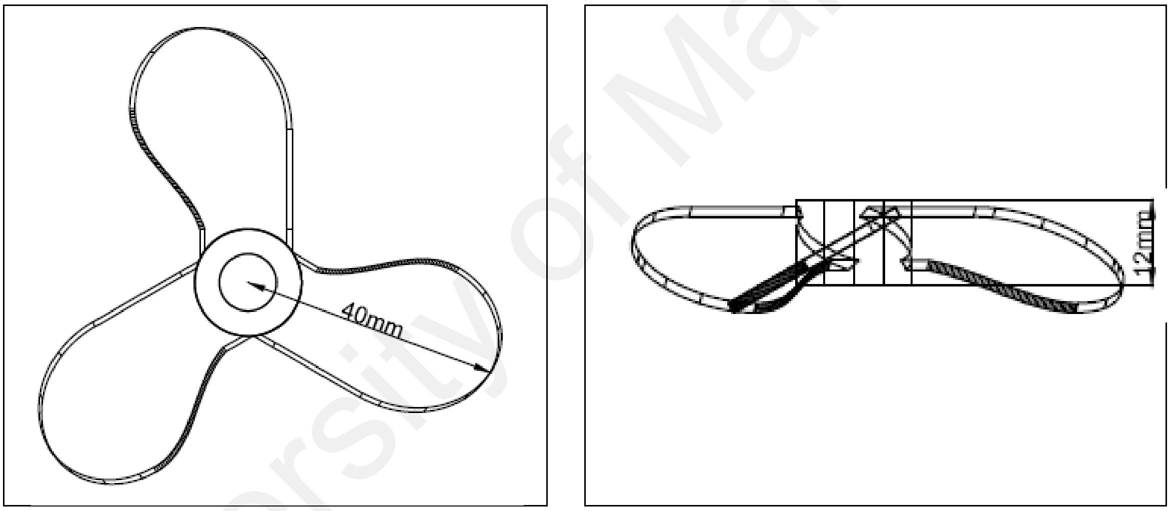

(a) (b)

Figure 3.4: Schematic diagram for 3P (d80), 25° pitched blade
(a) top view; (b) side view

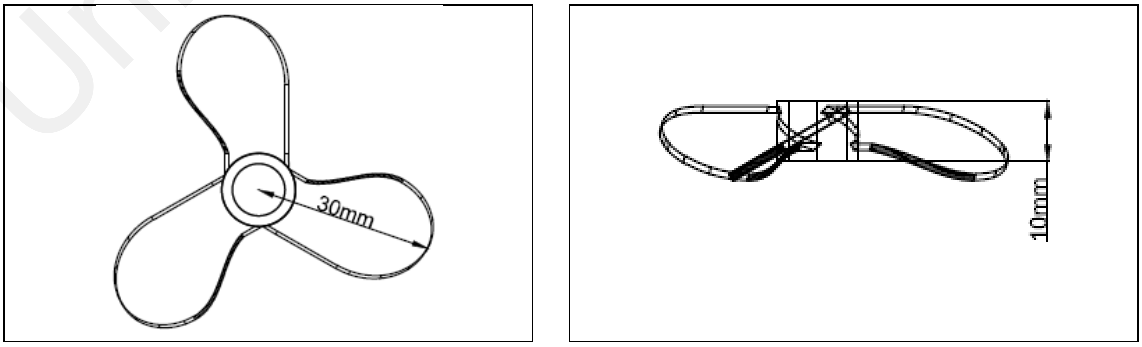

(a) (b)

Figure 3.5: Schematic diagram for 3P (d60), 25° pitched blade
(a) top view; (b) side view

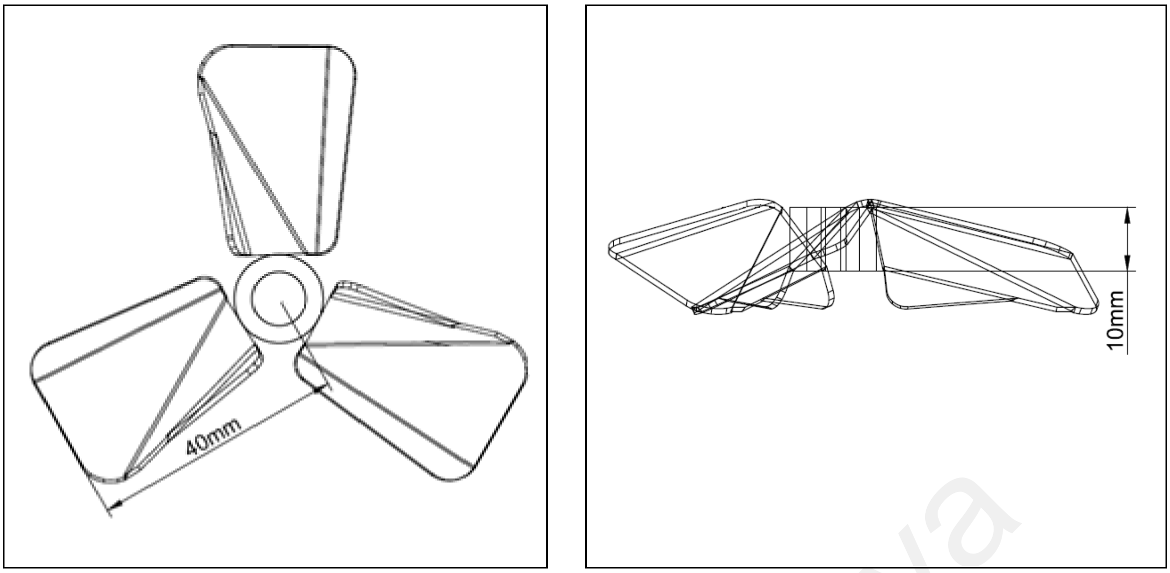

(a) (b)

Figure 3.6: Schematic diagram for HR100 (a) top view; (b) side view

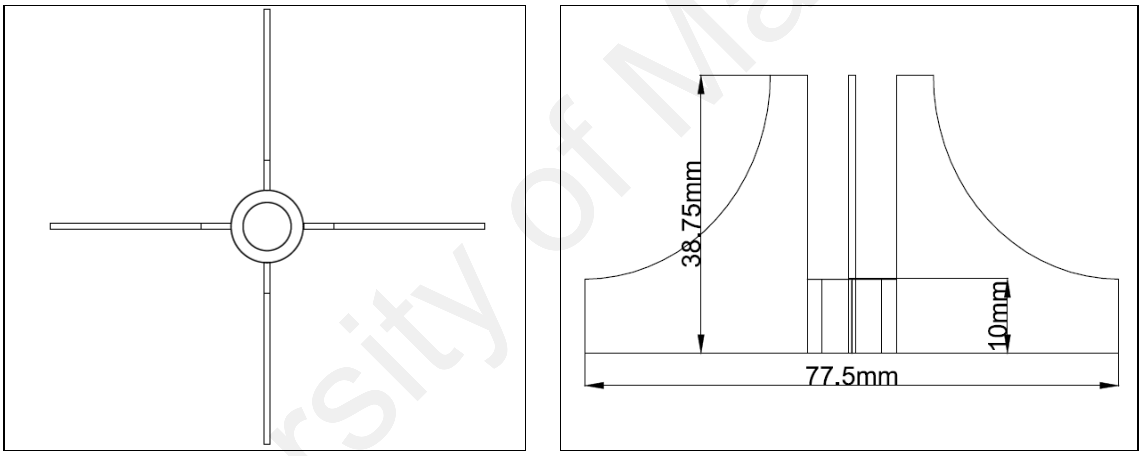

(a) (b)

Figure 3.7: Schematic diagram for HS604 (a) top view; (b) side view

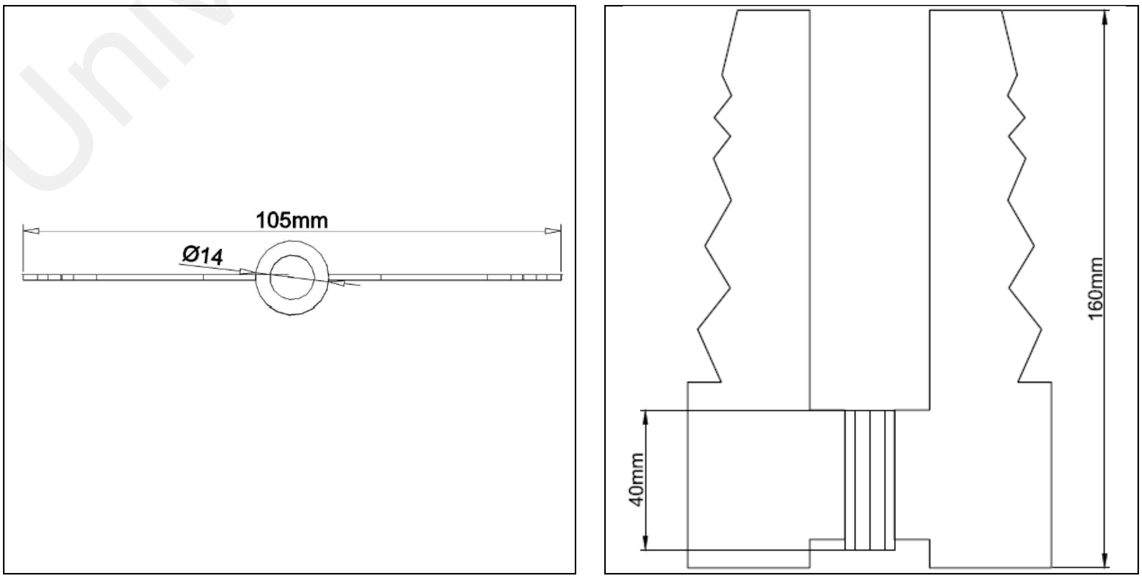

(a) (b)

Figure 3.8: Schematic diagram for MR203 (a) top view; (b) side view

Table 3.3: Impeller specifications

Impeller	4PBT	3P (d80)	3P (d60)	HR100	HS604	MR203
D/*T*	0.52	0.52	0.39	0.52	0.52	0.68
No. of blade	4	3	3	3	4	2
C/*D*	0.25, 0.50, 0.75, 1.00					
C/*T*					0.02	0.02
N_p	0.95-1.2	0.3-0.45	0.09-0.12	0.4-0.55	3.6-3.8	1.7-3.5*

* Taken in 2-baffled tank only

3.3 Power measurement

. Using the SATAKE® ST-3000II motor and torque transducer, impeller speed could be adjusted from the range 10-1500rpm. The impeller speed was increased gradually to lift the particles from the bed of solids. When the most of the solid bed was lifted, the last layer of particles remaining on the base will suspend and settle at a steady rate, but some will remain on the base. The speed was increased further to ensure no particles remained stagnant for more than 1-2s.

Torque was recorded for 10 min. and the average value was used to calculate power. Each reading is taken after mixing the slurry for 10 min. Two sets of torque reading were taken for each N_{js}, and error between the two readings must be within 5%. The torque, τ at N_{js} was used to calculate power at just-suspension, P_{js} using the relationship:

$$P_{js} = 2\pi\tau N_{js} /60 \qquad \text{-Equation (8)}$$

where

P_{js} is power in Watts

τ is torque in N·m

N_{js} is impeller speed at just suspension in revolution per minute (rpm)

Power per unit of total slurry mass gives the specific power consumption, ε_{js}. Specific power for at the just-suspended condition was calculated for justification of the impeller performance for solids suspension in this study. Power per mass of solids was also calculated and denoted as $P_{/}m_{s}$.

$$\varepsilon_{js} = \frac{P_{js}}{m} \qquad \text{-Equation (9)}$$

Where

ε_{js} is the specific power consumption, Watt/kg

P_{js} is the power at just-suspended condition, Watt

m is the mass of the slurry, calculated from apparent density, kg

3.4 Experiments in SATAKE, Japan

This project was carried out in collaboration with SATAKE Chemical Equipment MFG. LTD. (Japan). All the equipment including impellers and solid particles were provided by the company although experiments were all carried out at the University of Malaya (UM). A comparative study was also conducted with a dished base tank and the experiments were done by SATAKE in Japan. This thesis, however, only reports the work with a flat base tank done at UM. The only exception is the use of flow pattern sketches which was obtained by SATAKE Chemical Equipment MFG. LTD. (Japan) based on flow pattern observed from particles illuminated by a single-pulse NdYAG laser sheet fired in between baffles. The movement of tracer particle is observed on the light sheet fired on the tank.

3.5 Calculation of *S* values

S value is a geometric factor introduced in the Zwietering correlation (Equation (1)) to estimate the just-suspension speed of solid particles. Equation (1) is rearranged to calculate *S* values by substituting all known values of the variables.

$$S = \frac{N_{js} D^{0.85}}{\upsilon^{0.1} d_p^{0.2} (g\Delta\rho/\rho_L)^{0.45} X^{0.13}} \qquad \text{- Equation (10)}$$

Where

S is the geometric factor, to be calculated

N_{js} is the just-suspension speed (rps)

D is the impeller diameter (m)

υ is the viscosity of water, 0.001 Pa·s

d_p particle size (m)

ρ solid density - liquid density, $300 kg \cdot m^{-3}$

ρ_L liquid density, $1000 kg \cdot m^{-3}$

X is the concentration (%)

The S values are plotted against the impeller clearance and also tabulated to study how these values are affected by parameters in the equation such as particle size and concentration. The effect of change in clearance on S values is also included in this study.

CHAPTER 4

RESULTS AND DISCUSSION

4.1 Introduction

As described in Chapter 3 the just-suspension speeds, N_{js} under different conditions were determined directly from the experimental runs carried out with the range of impellers, clearances, particle sizes and concentration. At every N_{js}, torque measurement was made possible through a built-in torque transducer, and the torque was recorded at 10 min. interval. The torque values were used to calculate power at just-suspension, P_{js}, power per unit mass (total) or specific energy, ε_{js} as well as power per unit mass of solids only, P_{js}/m_s. The equations for calculating the power and specific energy are given in Chapter 3.

N_{js} data are presented in Figures 4.1 (a)-(d) as plots of N_{js} versus clearance for the four impellers 4PBT, 3P (d80), 3P (d60) and HR100. Specific energy (or power per unit mass) of these impellers are plotted against impeller clearance in Figures 4.2 (a)-(d). These plots are able to show the effects of clearance, particle size and concentration, and impeller geometry. The HS604 and MR203 were only used at one low clearance of 0.04*D*, so the N_{js} was plotted versus solids concentration as given in Figures 4.3 (a)-(b). Specific energy plots for these two impellers are shown in Figure 4.4 (a)-(b).Power per unit mass of solids is plotted against solids concentration in Figures 4.5 (a)-(f) to see if the optimum solids concentration can be identified for this work. Sections 4.2 to 4.5 discuss these trends, and the deductions that can be made from their analyses.

In the process of determining N_{js} by visually ascertaining Zwietering's criterion, particles distribution on the base inevitably had to be scrutinized. Since a trend to the distribution behaviour was repeatedly observed, it was worth to have it carefully recorded and related to the quantitative data. Section 4.6 is dedicated to this effort. This observation is supported by flow pattern measurements using a laser technique particle tracking velocimetry (PTV) that enables the pumping pattern of the impeller to be drawn out to provide explanation corresponding to the particles flow behaviour on the base.

Finally, since this entire work has been based on the Zwietering's method and criterion, Section 4.7 is devoted to the *S* factor which is the constant that makes Zwietering equation works under the different conditions. When the equation was first published, *S*, known as the geometric factor was described to be a function of the geometry, namely impeller type and clearance. However, research has shown that the *S* factor is dependent on many other variables including solid properties (Ibrahim et al., 2012). Since N_{js} have been determined for numerous conditions here, this work would not be complete without applying the data in Zwietering's correlation to generate the values of *S* under the different conditions. Analysis of the *S* values will show the range over which the value remains reasonably constant, that it can be maintained for use in the equation for the prediction of N_{js}.

4.2 Effect of Clearance

It is generally expected that increasing the impeller clearance from the tank base would require higher speed and energy to achieve suspension under otherwise similar conditions, since the fluid has to travel a greater distance after being discharged from the impeller and some momentum would be lost before reaching the tank base to lift the particles.

Figures 4.1(a)-(d) illustrate the effects of clearance on N_{js} for four impellers of the axial type, with the three particles sizes and over the range of concentrations studied. It should be noted that for the same C/D, a larger impeller diameter means a higher clearance. Of the four impellers studied here, only the 3P (d60) has a smaller diameter while the other three have the same diameter of 80mm. Hence, the actual clearance at C/D=1.00 for the 3P (d60) is equivalent to actual clearance at C/D=0.75 for the 80mm impellers. In other words, for the same C/D, 3P (d60) is actually placed closer to the tank base. Naturally the speeds required to cause suspension are also higher for the smaller impeller when compared at the same C/D as the larger impellers.

General observations of the N_{js} plots show that:-

(i) N_{js} increases with clearance, but for 4PBT and 3P (d80), the increase in N_{js} between clearance 0.25 and 0.50 can be very small. In fact, a slight decrease of N_{js} is seen for these impellers when suspending the MW particles.

(ii) The HR100 is least affected by clearance for all particle sizes, as evidenced by the lowest slope gradients amongst all the plots. In suspending the SW particles, from C/D = 0.75 to 1.00, the N_{js} increment for HR100 is less than at the lower clearances.

(iii) The N_{js} in HR100 is the lowest compared to all other impellers. The just suspension speed to suspend MW particles is also relatively low with 4PBT and 3P (d80)

Figures 4.2(a)-(d) illustrate the effects of clearance on the specific energy (power per unit of total mass) at just-suspension, ε_{js} for the different impellers used in this work. The plots on the effect of clearance on power requirement are shown in Appendix C as the trends for both power and specific energy plots are almost identical. This could be because the denominator (total mass) used to calculate the specific energy only varies less than 2%, in going from 5wt% solids to 40wt% solids. Hence, effectively it is like the power values are being divided by a constant in going from P_{js} to ε_{js}. In analyzing the ε_{js} graphs (Figures 4.2(a)-(d)), the following can be observed:-

(i) Increasing the clearance from 0.25*D* to 0.50*D* required very little or no increase in specific energy for suspension. In fact ε_{js} is slightly lower at the clearance of 0.50*D* than at 0.25*D* for the 4PBT.

(ii) Increasing the clearance beyond 0.50*D* led to significant increase in ε_{js} with the highest specific energy requirement being at the highest clearance of C/D=1.0 for the 4PBT and 3P (d80).

(iii) The HR100 and 3P (d60) were almost unaffected by clearance change

Similar to the findings by Ayranci and Kresta (2011), the effect of impeller clearance depends on the impeller type and also the particle properties. This is also seen in Figures 4.1 and 4.2 that the change in N_{js} and ε_{js} with clearance vary with the type of impeller, particle size and concentration.

Clearance effect is significant for pitched blade impeller (4PBT), compared with the 3P (d80) and HR100. Ayranci and Kresta (2011) reported the hydrofoil impeller, Lightnin A310 and the 4 bladed pitched blade turbine had similar N_{js}. However, the P_{js} of the pitched blade impeller extended from two-times of the A310 at the lowest clearance investigated, to four-fold at the highest clearance. A HE-3 impeller of similar D/T requires a much higher impeller speed to suspend glass beads, but it is slightly more energy efficient to suspend glass beads than a six-bladed pitched blade impeller (Ibrahim & Nienow, 1996). Jirout and Rieger, (2012) finds that among the impellers used in their study, the propeller is more sensitive to the clearance.

4PBT is a mixed flow impeller while 3P (d80) and HR100 are axial impellers; 3P (d80) has higher ε_{js} than 4PBT. According to Sharma and Shaikh (2003) and Ibrahim and Nienow (1995), flow pattern of axial impellers changes from single-eight to double-eight at a clearance C/T>0.35 (≈0.70D). All the axial impellers used in this work give a hike of ε_{js} at a clearance 0.75D. As an axial impeller, the increase of ε_{js} at a similar change in clearance is minimal compared with 3P (d80) and 4PBT. The blades of the HR100 generate a strong axial flow regardless of the impeller clearance. This flow characteristic makes HR100 advantageous to clear particles from accumulate on the centre base, even at high impeller clearance of 1.0. Therefore, it is understood that the effect of flow characteristics of HR100 that contributes minimal dependency in power demand and solids concentration, particularly at high impeller clearance.

Despite the difference in N_{js} at increasing C/D, the ε_{js} for the propeller of D/T =0.39 is more stable than the impellers of D = 0.52T. Gray (1987) reported that for C> 0.35T, the flow under the tank changes from axial-flow to a flow pattern similar to one generated by a radial impeller. It could be found in the 4PBT and 3P (d80), at C>0.75D (≈0.39T), there is a higher increment in the ε_{js}. As C/D for this study uses impeller diameter as reference (denominator), the 3P (d60) propeller is actually placed closer to the tank base than 3P (d80). For example, C/D=1.00 for 3P (d60) is equivalent to C/D=0.75 for 3P (d80), which just reached the third region reported by Gray (1987). This explains the constant ε_{js} value for the 3P (d60) compared to 3P (d80).

In general, placing the axial impeller closer to the tank allows the flow to interact with the tank walls, creating a more energy efficient particles suspension in the solid liquid system. Experimental results for the range of axial impeller studied come in good agreement with the finding of Chapple et al. (2002). Other factors such as the impeller geometry, particles properties and C_w could be amplified at if the system is operated at high clearance.

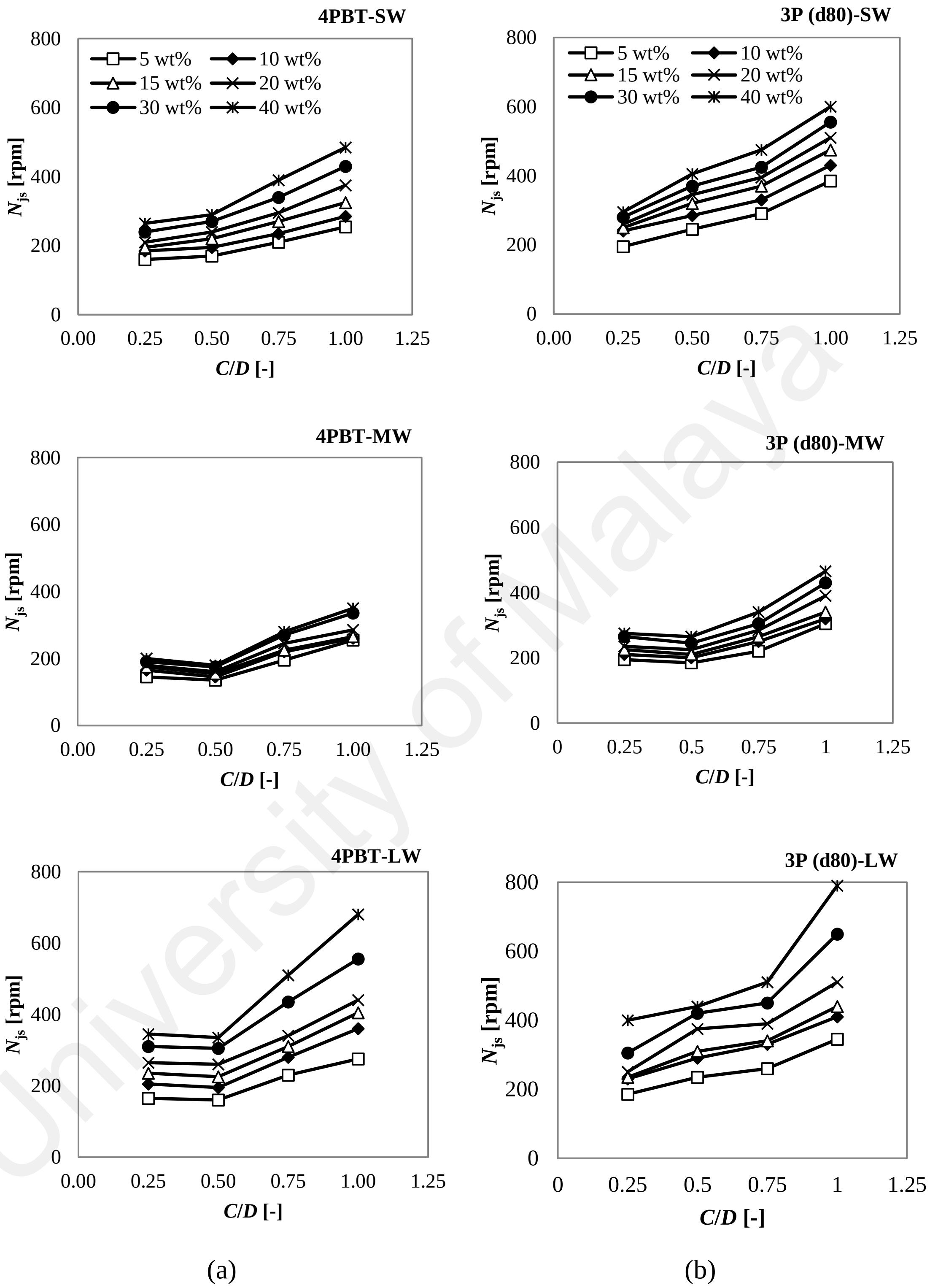

Figure 4.1: The effect of clearance on N_{js} (a) 4PBT; (b) 3P (d80)

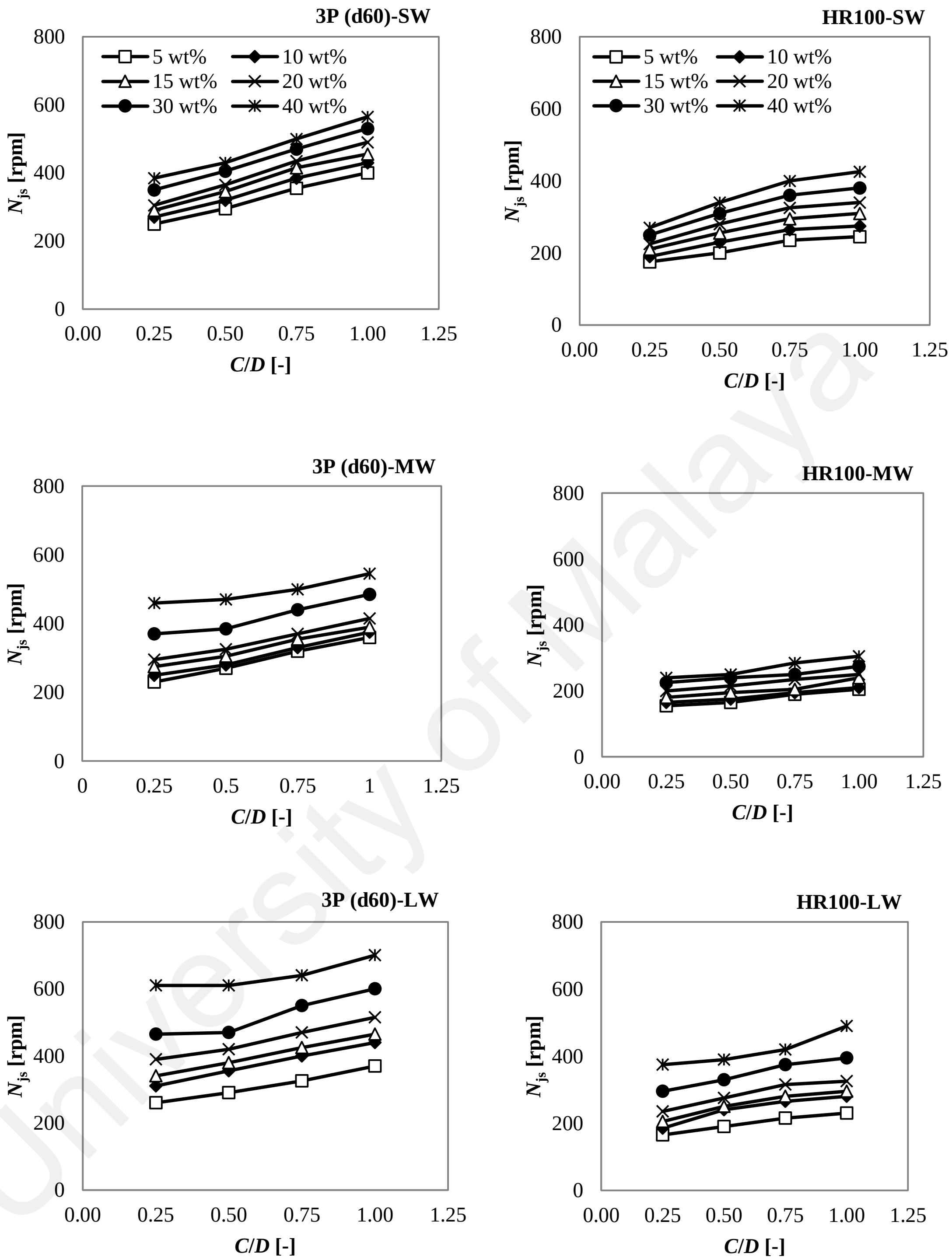

(c) (d)

Figure 4.1, continued.: The effect of clearance on N_{js} for (c) 3P (d60); (d) HR100

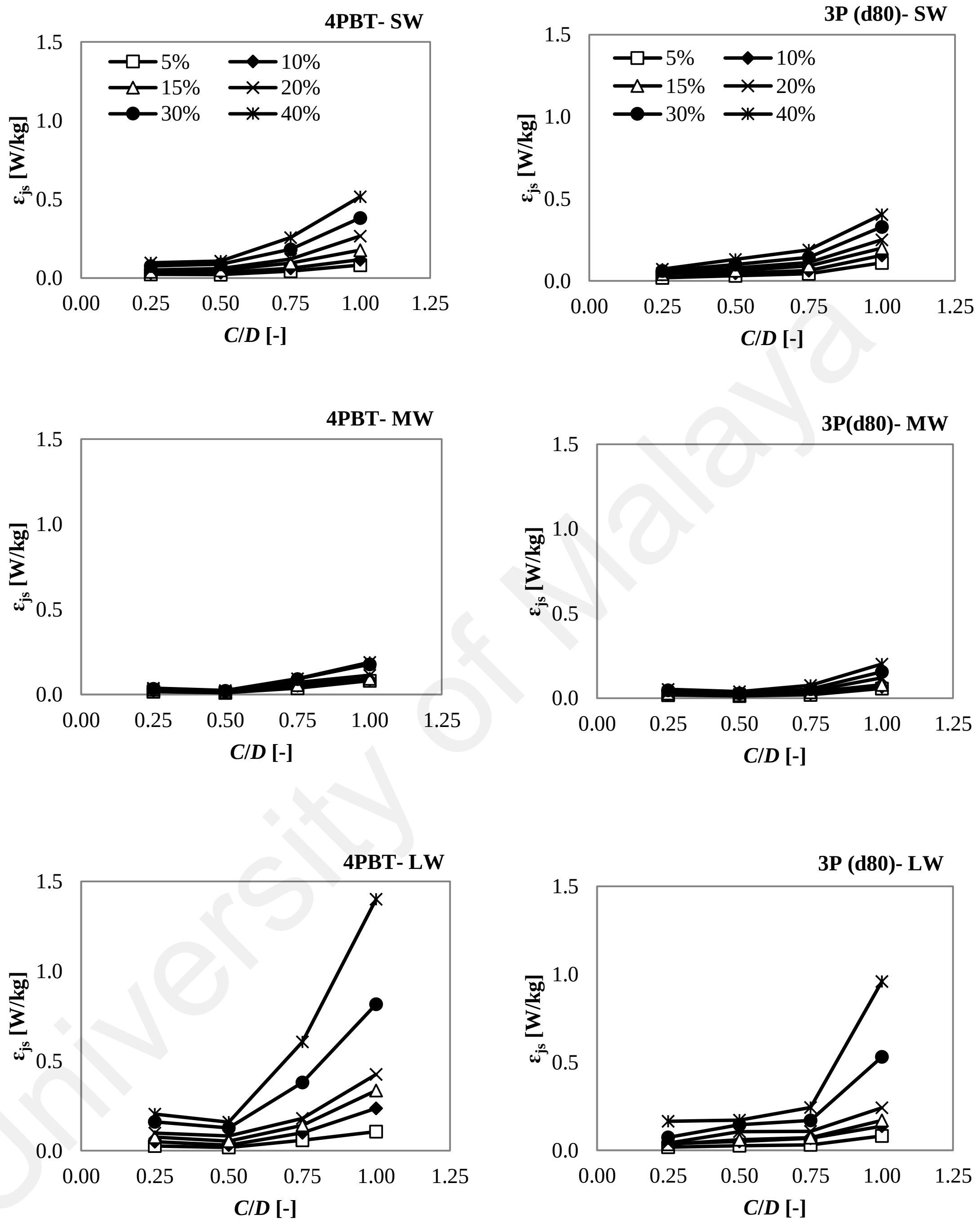

(c) (d)

Figure 4.2: The effect of clearance on ε_{js} for (a) 4PBT; (b) 3P (d80)

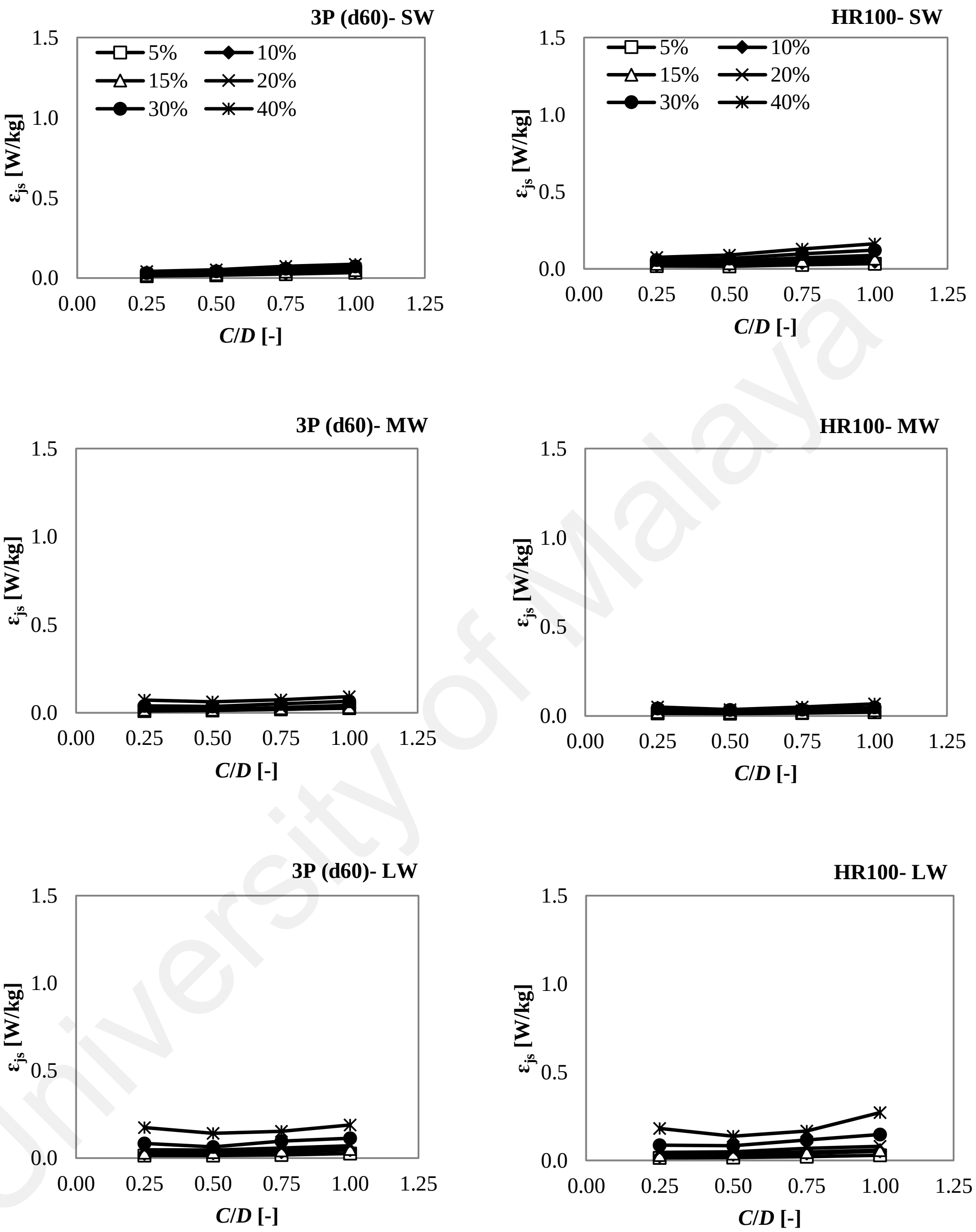

(c) (d)

Figure 4.2, continued: The effect of clearance on ε_{js} for (c) 3P (d60); (d) HR100

4.3 Effect of particle size

The effect of the particle sizes can also be observed from Figures 4.1(a)-(d) and 4.2(a)-(d).

(i) It is interesting to highlight from Figure 4.1 that the medium-sized particles (MW) required the lowest minimum speed and specific energy for just-suspension.

(ii) The N_{js} and ε_{js} of the medium-sized particles (MW) are also the least affected by clearance, while the largest particles (LW) just-suspension is most affected by impeller clearance, followed by the smallest particles (SW).

(iii) Stagnant particles was not found in SW, but its presence was to be observed at >15wt% for LW.

(iv) Another observation is that for LW and SW the effect of particle concentration is more pronounced with higher clearance, particularly at C=D. This is especially true for the 4PBT and 3P (d80). At this clearance, the ε_{js} for both 3P (d80) and 4PBT are strongly affected when the concentration increased from 20wt% to 30wt% and 40wt%. Hence, at higher concentrations, the ε_{js} difference with clearance is more pronounced. ε_{js} for both 3P (d80) and 4PBT doubled at C/D = 0.75 and C/D=1.00. Though 3P (d60) and HR100 experience a similar change in ε_{js} at these concentrations, the increment is minimal compared to the 3P (d80) and 3P (d80).

(v) In this work, solids of the smallest diameter were observed to be more compact, as though the particles goes through a "consolidation" process. SW particles lighter as individual particles, and the movement of these particles are more easily affected by the turbulence in the system. It is observed that the particles often move in different directions, and the movements are easily affected by the flow. A longer time was required before the system achieved steady state to ascertain the N_{js}. After sedimentation, solids had a smooth pasty texture compared to grainy texture of the larger particles. However, both appears to be water-like slurry when all particles are well suspended. Although the small diameter coupled with low density of the PMMA meant the particles took a long time to settle in the tank once suspended, stirring the settled solids was a challenge, particularly at high concentrations. The impeller had to be set at higher *C*/*D* to loosen the top layer of the solids prior to lowering it down to the desired operating *C*/*D*. If the impeller was buried in the settled SW particles, it could not be rotated.

At high concentration, MR203 and HS604 are partially immersed in the settled solids. N_{js} for in all experiments using these two impellers are stable, ranging between 100-250rpm.

The ε_{js} of 4PBT, 3P (d80), 3P (d60) and MR203 are more sensitive to the change in particles size of the same concentration, especially at the highest concentration (40wt%) and clearance.

Higher ε_{js} is needed to suspend the LW particles than the smaller particles. ε_{js} to suspend SW and MW particles are similar for the 3P (d60) and HR100 impellers, and these two impellers has lowest ε_{js} among the impellers. In the LW slurry, the 4PBT impeller required a much higher ε_{js} than the other impellers.

HS604 and MR203 are impellers of low mixing speed. Both impellers have relatively similar speed increment for all experiments performed, as shown in Figures 4.3(a) and (b). ε_{js} of HS604 is much lower compared to MR203, though change in particle sizes shows little effect on ε_{js} (Figures 4.4 (a) and (b)) and N_{js} of both impellers.

HS604 has relatively low N_{js}, this is more notable at high concentrations. A very low clearance setting of the impeller created strong flow, making the particles suspend more easily, especially with the large d_p. With this impeller the effect of particle size on N_{js} is less pronounced than the other impellers.

Brownian motion are only significant in the hydrodynamics when d_p<1 µm. These particles induce hydrodynamic disturbance of the flow field in a liquid media, which increases the energy dissipation and viscosity (Zhou, Scales & Boger, 2001). There is also a possibility for changes in slurry properties such as the rheology as the SW particles are being dispersed in the liquid phase, high concentration of its fine texture could affect the particle-liquid and particle-particle interactions.

Wang et al. (2012) had shown that ε_{js} reduces with smaller particle size range, but for particle sizes below 120 µm, there was a tendency for ε_{js} to increase. The ε_{js} for the same concentration is very different with different particle sizes. In the 40wt% slurry, the ε_{js} for the LW could be as high as four-fold of MW (Figure 4.2 (a)) while the ε_{js} for the SW could be double of the MW. Higher N_{js} and ε_{js} at increasing d_p is explained with the higher particle settling velocity in larger particle size (Ochieng & Lewis, 2006; Wang et al., 2012, Atiemo-Obeng et al., 2004). This explains why the ε_{js} using the LW is much higher than MW, but not for the ε_{js} of SW.

Particles of same density are used in all experiments, and the only variable is the d_p. The amount of particles present per unit weight of solid particles, would be more in the smaller-sized particles compared to the larger ones. This gives a larger total surface area, which is favourable in mixing for reactive systems when area for particle-liquid interaction increases and more chances for particle-particle collision. It is suggested that the particle settling velocity is the factor that dominates the effect of particle size when the difference between the particle sizes is big. A critical size could be present in the particles where mass difference between the particles is so small that the particle-particle interaction taking place in the reactor has more significance than the terminal settling velocity.

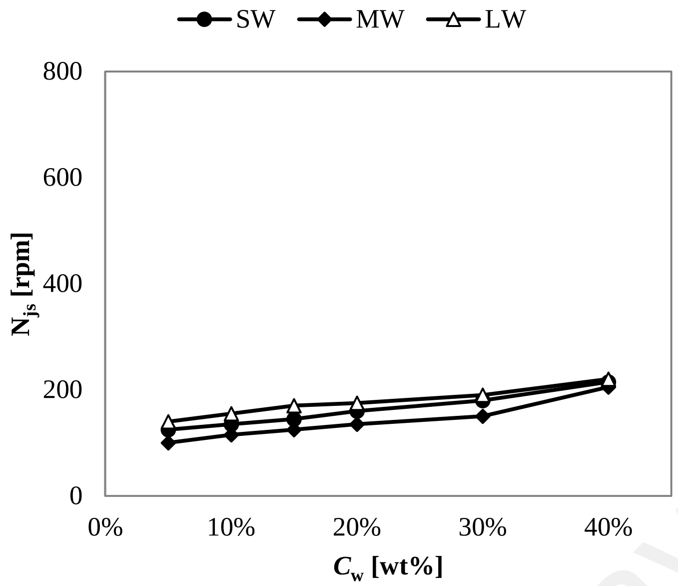

(a)

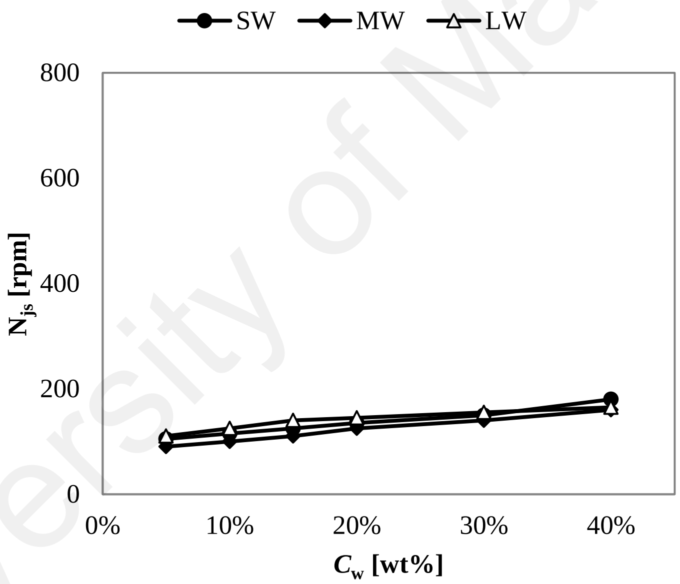

(b)

Figure 4.3: The effect of concentration on N_{js} in (a)HS604; (b)MR203

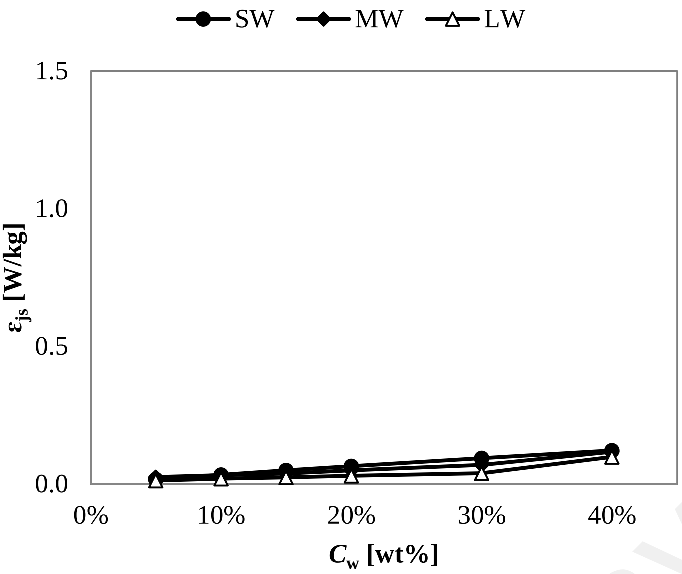

(a)

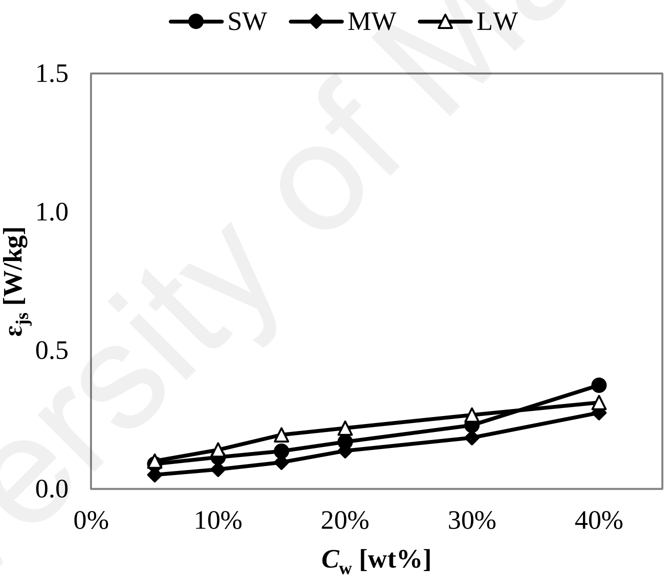

(b)

Figure 4.4: The effect of concentration on ε_{js} in (a) HS604; (b) MR203

4.4 Effect of solids concentration

Generally, N_{js} and ε_{js} increases with increasing concentration. In this work, much higher energy is required to suspend particles in concentration above 30wt%. Especially at C=D. 0.75 and 1.0 onwards, where the discharge flows tend to lose momentum at higher clearance.

Earlier works suggested that the steep increment of ε_{js} at high solids concentration is due to the particles interaction which is significant to the present study (Ayranci et al., 2013; Bubbico et al., 1998; Wang et al., 2012). The interactions includes particle-liquid interaction, particle-particle interaction, or particle reactor interaction. Energy loss in the form of friction occurs in these interactions. This study shows that much more energy is required when the concentration is increased up to 30-40wt%, approximately double of that in 20wt%.

Figures 4.5(a)-(f) show the effect of solids concentration on the power per unit mass of solids (P/m_s). P/m_s is an expression of normalizing power input for just suspension condition to the solids mass. An optimum concentration at where the minimization of P/m_s is present, which is important to maximize product throughput by operating at higher solids concentrations. Hence, at concentrations below the optimum solids concentration, power supplied into the system is not fully utilized (Wang et al., 2012). For all impellers studied in this work, power consumption hits minima at 15-20wt% of solids.

At lower clearances, increasing the solids concentration only gives minor effect to the values of P/m_s, compared to the higher clearances. From C/D 0.50 to 0.75, P/m_s

increased to two-fold to that of clearance 0.50. The difference of P/m_s between clearance is consistent throughout all concentrations for a given particle size.

Power consumption for 4PBT and 3P (d80) is easily affected by the change in particle size and clearances. At high clearances and large particles, P/m_s increases immediately after the minima is achieved, especially with 3P (d80). These impellers are only fit to be used at a small range of concentrations. As concentration increased up to 40wt%, P/m_s is higher than the large impeller, MR203. For other impellers, effect of the solids concentration is less pronounced. Power consumption gradually decreases until it reaches 20wt%, and slightly goes up at 30wt% or remains at the minima till the highest concentration.

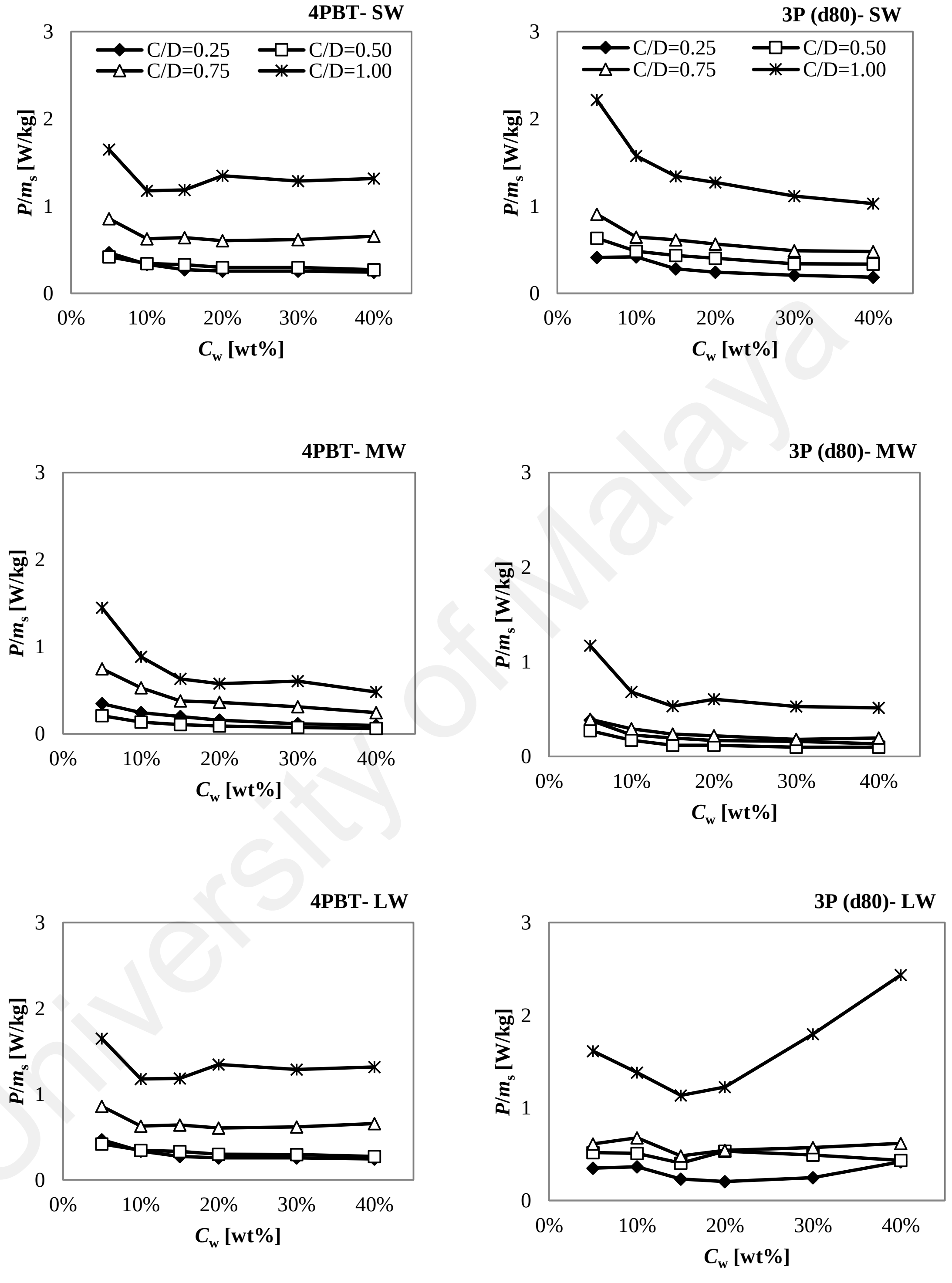

(a) (b)

Figure 4.5: The effect of concentrationonpower per unit mass of solidsfor (a) 4PBT; (b) 3P (d80)

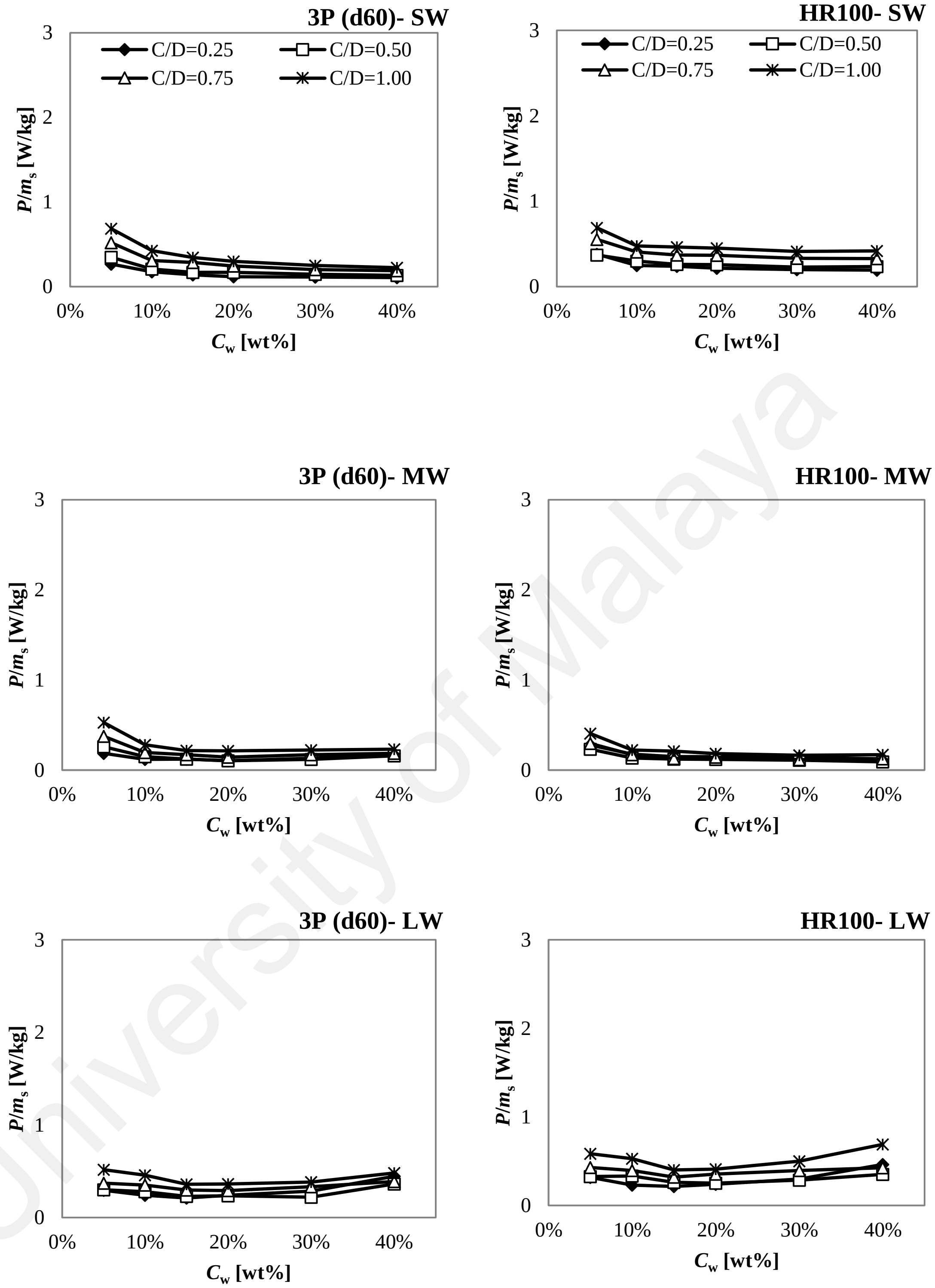

(c) (d)

Figure 4.5, continued: The effect of concentration onpower per unit mass of solids for (c) 3P (d60); (d) HR100

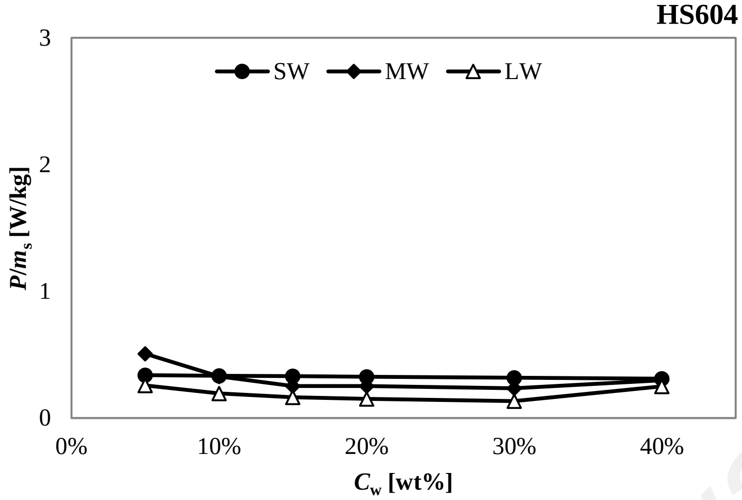

(e)

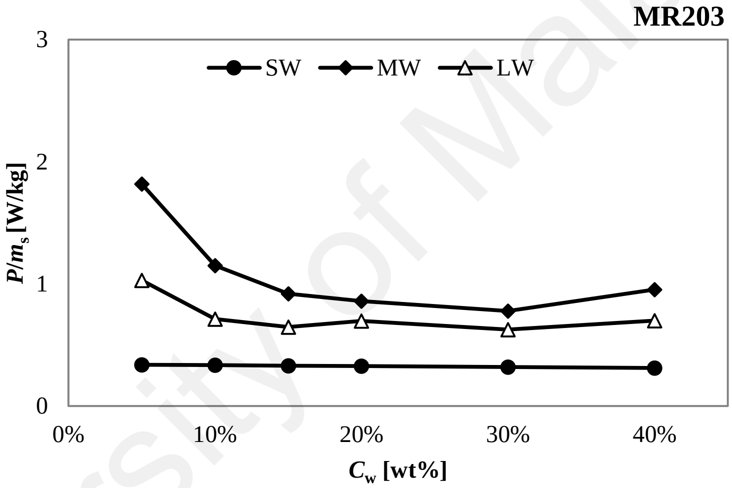

(f)

Figure 4.5, continued: The effect of concentration onpower per unit mass of solids for (e) HS604 (f) MR203

4.5 Comparing impeller performance

A main objective of this work is to compare the performance of novel impeller designs by SATAKE Chemical Equipment MFG. LTD. over conventional designs. N_{js}, ε_{js} and P/m_s were used to compare the energy efficiency of the impellers for solids suspension in stirred tank.

It is found that the novel impellers, HR100 and HS604 exhibited relatively lower power consumption. The HR100 design has the added advantage of being less affected by clearance and solids concentration. The standard 3P (d60) has comparable efficiency while the other conventional impellers are significantly less efficient. The HR100 and 3P (d60) have a relatively low ε_{js} for all studied clearances, and theε_{js} in these impellers is least affected by change in clearances. The ε_{js} difference as the clearance moved on from 0.50D to 0.75D is as high as 5 times for 4PBT and 3P (d80), whereas in HR100 and 3P (d60), the ε_{js} is only doubled even with the highest concentration slurry. Yet, comparing at an equivalent clearance for 3P (d60) at clearance 1.00 and HR100 at clearance 0.75, it can be observed that the ε_{js} is higher for 3P (d60), making HR100 the impeller that is least affected by clearance.

4PBT has similar ε_{js} at clearance 0.25 and 0.50, a hike in the increment is observed from clearance 0.75 onwards. 3P (d80) has similar increment of ε_{js} for clearance 0.25-0.75, but observed to increase drastically at clearance 1.00. It is observed that the double loop flow pattern is present in the stirred tank at clearance 0.75 for the 4PBT and clearance 1.00 for the 3P (d80), respectively. The presence of this double-loop radial flow increased the ε_{js} for solids suspension. Only partial energy is delivered to these secondary circulation loops for solids suspension (Raghava Rao et al., 1988). ε_{js} at clearance 1.00

can be four-fold of clearance 0.75 and 0.50 for the 4PBT and 3P (d80) impellers, respectively.

Both HS604 and MR203 with low clearance setting operates at low impeller speed and has low N_{js}, HS604 has much lower ε_{js}. Nienow (1968) suggests that solids suspension is efficient with large impellers at low clearance, however findings from this study show that the large impeller MR203 does not excel in solids suspension. The impeller design shall be the main factor that governs the impeller performance in solids suspension.

The HR100 and HS604 are most energy efficient at the highest concentrations and the largest particles, LW. The HS604 is also the least affected by the changes of solids concentration as compared to the other impellers, although using HS604 in SW and MW requires slightly higher energy.

The HR100 and 3P (d60) require much less specific energy than the other two impellers, however for the 4PBT and 3P (d80) the specific energy for MW particles are very low; equivalent to those with HR100 and 3P (d60).

MW is least affected by concentration and clearance for all impellers studied. The effect of clearance is more pronounced in suspending LW and SW particles, especially with the 4PBT and 3P (d80) impellers. Effect of d_p is more consistent with MR203, where change in particle sizes will have similar effect throughout all concentrations. This impeller covers about 70% of the tank base surface and the suction force easily lifts the particles at the tank base. However this impeller has high power consumption, even in suspending particles of low concentration. HR100 and 3P (d60) have similar ε_{js} for all particle sizes until the solids concentration is increased from 30wt% to 40wt%, when the effect of particles sizes becomes more notable. HS604 is least affected by particle size among all impellers, ε_{js} is very similar for the different particles used at all studied concentrations. The radial flow created at the tank base easily sweeps the solids off the base, even in high concentration.

Solids concentration has important effects on the ε_{js} and P/m_s for 4PBT, 3P (d80) and MR203 impellers while 3P (d60), HR100 and HS604 is less affected. Nevertheless the graphs show that it would not be the most optimal to suspend solids at low concentrations (below 15-20wt%) for all impellers. The only exception is for 3P (d80) at C/D=1.0 where P/m_s increased after 20wt% of LW solids; hence, in this case the optimum solids concentration for operation is limited to the range between 15-20wt%. The HS604 requires low power consumption for full range of solid concentrations among all impellers.

4.6 Flow patterns

The flow patterns of the different impellers were recorded by observing movements of tracer particles on the laser sheet fired with a NdYAG laser. The flow patterns for the 4PBT, HR100 and 3P (d80) were observed at 4 clearances, and HS604 at single low clearance of 0.02*T*. All impellers are set to rotate at 150rpm. The flow pattern observed on the light sheet is considered in explaining particle distribution on tank base. As discussed by Ibrahim and Nienow (1996) flow pattern generated by impeller pumping could explain particles distribution on the tank base.

Figure 4.6 illustrates the sequence of how the solid particles are lifted from the base of the tank. It is clear that the impeller design, impeller clearance from the base, and particle size have significant effect on how the solid particles are suspended and the location where the particles are last suspended. In one case the particle concentration also appears to make a difference. These are important to note as it could directly be related to the energy required for suspension. In analyzing the distribution patterns shown by Figure 4.6, a few observations can be highlighted. Firstly, the particle distribution on the base is generally similar for all particle concentrations within a single clearance. Secondly, particle distribution at the tank base is more consistent throughout all the clearances with the HR100, compared to the 4PBT and 3P (d80). Interestingly, the HR100 was observed to produce consistent particle distributions for SW and MW experiments, but different with the LW. Thirdly, the last point of suspension for the 4PBT was always at the tank centre. This could be due to the diameter of 4PBT used being 0.52, and Ibrahim and Nienow (1996) had shown that for the pitched-blade impellers, solid particles are suspended from the centre if the impeller to tank diameter ratio is about 0.52, while a D/T of 0.33 led to the last point of suspension occurring at the periphery of the base.

A phenomenon that occurred with the MW and LW particles but not the SW, is "moving on the spot", or the lack of mobility while particles "vibrate" in place. This was observed throughout the range of the impeller speed, with a small portion of particles remaining fixed in certain areas of the base. Since the amount is extremely small and it was almost impossible to get them to move, they are overlooked for the purpose of determining N_{js}. The SW particles on the tank base were very much affected by the recirculation loops that caused flow in the reverse direction to the main pumping direction. When caught in the meeting of the opposing flows the MW and LW particles appeared to remain stagnant but were in fact vibrating their own position without being moved much to a different spot. This has also been observed with BLGB (Ibrahim & Nienow, 1999) in more viscous fluids. Even though the BLGB used were much larger in size, their density was also almost two times higher which could explain this condition of being trapped between flows from different direction, thus restricting the mobility.

The details of solid particles distribution according to geometry are given in the following sub-sections.

<table>
<tr><td rowspan="2">Impeller
(D/T=0.52)</td><td colspan="9">Particle Size</td></tr>
<tr><td colspan="2">SW</td><td colspan="4">MW</td><td colspan="3">LW</td></tr>
<tr><td>4PBT

C/D</td><td>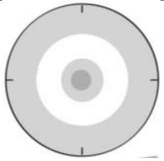
0.25, 0.50</td><td>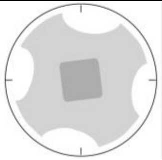
0.75, 1.00</td><td colspan="2">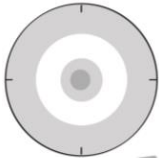
0.25. 0.50</td><td colspan="2">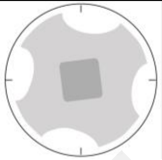
0.75, 1.00</td><td colspan="2">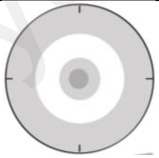
0.25, 0.50</td><td>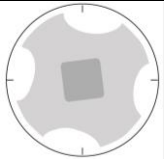
0.75, 1.00</td></tr>
<tr><td>3P (d80)

C/D</td><td>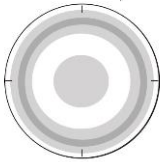
0.25, 0.50, 0.75</td><td>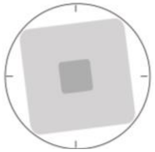
1.00</td><td>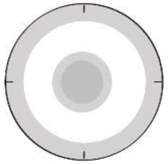
0.25</td><td colspan="2">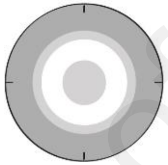
0.50</td><td>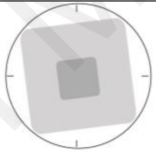
0.75, 1.00</td><td>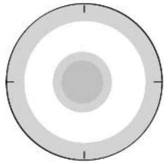
0.25,0.50</td><td>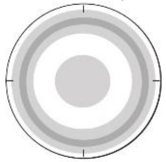
0.75</td><td>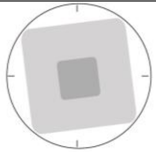
1.00</td></tr>
<tr><td>HR100

C/D</td><td colspan="2">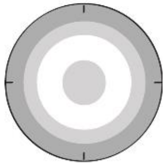
All C/D</td><td colspan="4">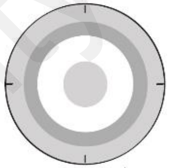
All C/D</td><td>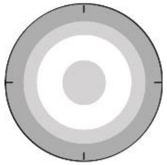
0.25</td><td>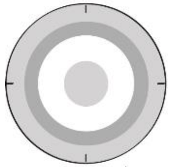
0.5, 0.75, 1.00</td><td>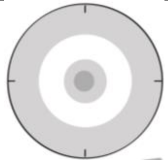
1.00
(40wt% only)</td></tr>
<tr><td>HS604

C/D</td><td colspan="2">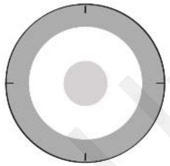
0.04</td><td colspan="4">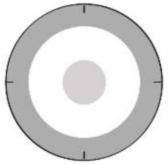
0.04</td><td colspan="3">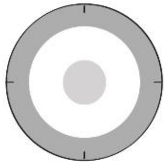
0.04</td></tr>
</table>

**Intensity of color represents the order of the particles suspended, with darkest color as the last point of suspension.*

Figure 4.6: Sequence of particle distribution on a flat-based tank (T=155mm)

4.6.1 Flow pattern for 4PBT

The impeller discharges towards the bottom of the tank at an angle that is less axial than the 3P (d80) and HR100. At the lower clearances of 0.25 and 0.5 the downward pumping tends to push the tracer particles to the side of the base, but since the impeller diameter is large relative to the tank base and the pumping direction has a significant radial component, a weak flow zone occurred below the impeller hub. In observing the flow pattern, tracer particles were observed to be moving weakly at the tank centre; some seem to be moving upwards while others were observed to fall back to the tank bottom. Larger solid particles remained longer at the centre of the base, and became the last particles to be suspended.

As the clearance was increased, the weak central zone is fed with more tracer particles as secondary recirculation flow formed with the higher clearances pushed particles inwards on the base. While some tracer particles were observed to be weakly drawn upward at C/D=0.50, others were observed to fall back to the base or drifting with the dominating flow direction.

As the clearance is increased to 0.75, the secondary flow formed below the impeller is larger and at clearance 1.00, the loop size is similar to the main discharge flow. Hence, at these high clearances the flow pattern changed from a single-loop to double-loop. At each increasing clearance the flow below the impeller gets more unsteady and movement of the tracer particles consistently changed with time, depending on the flow that dominated. At the central region close to the base, the flow is even weaker and only hits the base occasionally. Accumulation of tracer particles occurred on the base. The accumulating tracer particles move in a swirling motion, clock-wise (same as impeller direction), with only occassional weak-lifting movement is observed in the particles.

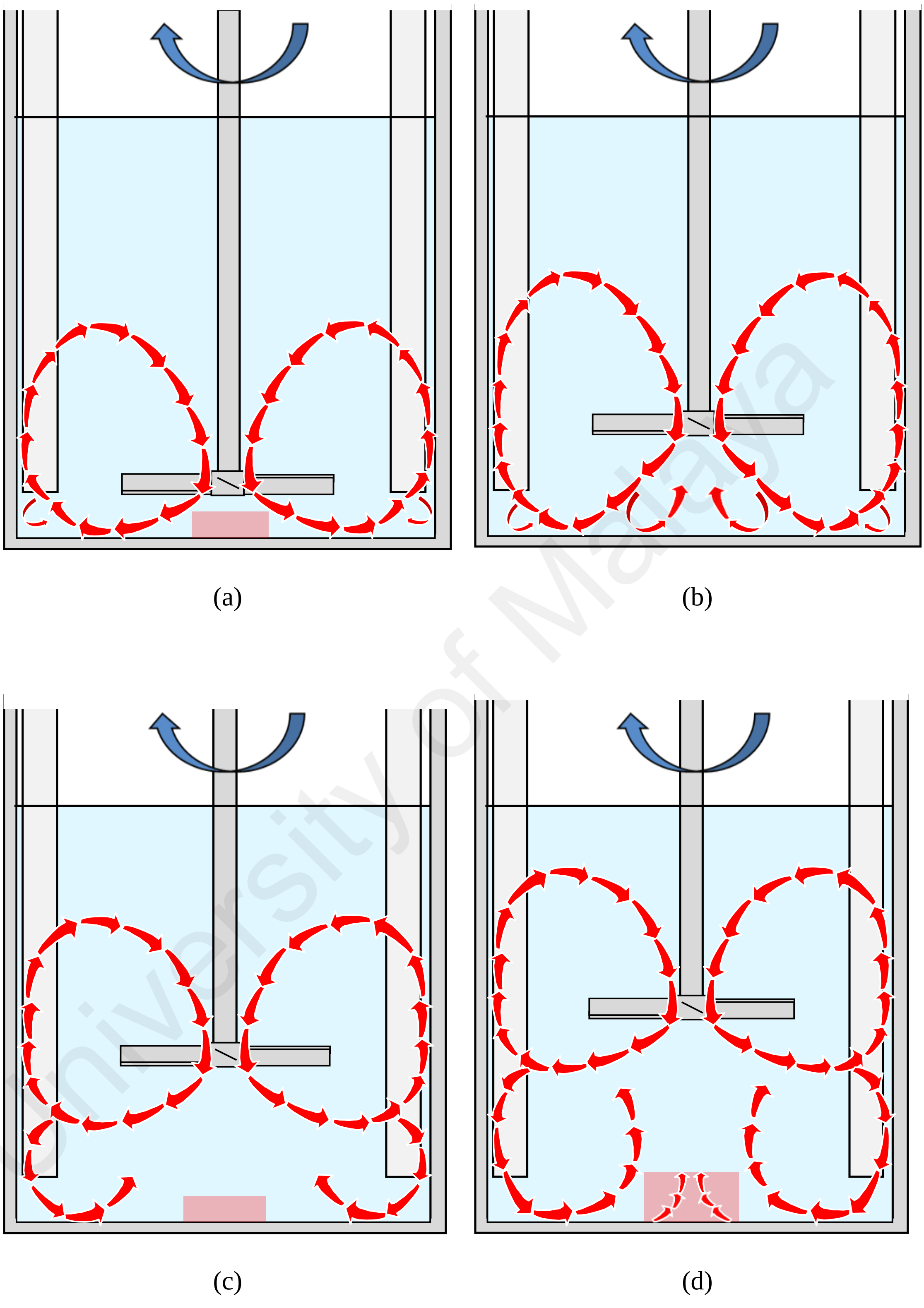

Figure 4.7: Flow pattern in 4PBT (a) C/D = 0.25; (b) C/D = 0.50; (c) C/D = 0.75; (d) C/D = 1.00

The observed flow pattern explains the particle distribution observed on the tank base. As mentioned in the preceding paragraph, for all experiments using the 4PBT, the last point of suspension is the tank centre. At the lower clearances (0.25 and 0.50), the particles are lifted first from the annular region. Instead of particle accumulation often found at the baffle base, solid particles are first lifted from the sides for clearance 0.75 and 1.0. In some experiments, the solid particles could be observed to be lifted in a swirling movement before N_{js} is achieved. The positions of these swirling flows could be located randomly at different position of the central region. Generally, N_{js} for clearance 0.50 is similar to the clearance 0.25.The flow present under the impeller at clearance 0.50 helps to lift the particles at the tank centre, which also explains why MW particles are lifted with slightly lower N_{js} at the clearance 0.50.

The double-loop flow at clearance 0.75 and 1.00 is similar to the flow of a radial impeller (Sharma & Shaikh, 2003; Ibrahim & Nienow, 1995). From this point onwards, ε_{js} shows a sudden increment, as though the impeller is behaving like a radial impeller, which is known to be inefficient for solids suspension. In fact the clearance of four areas on the side of the base is akin to the "star formation" described for the radial Rushton turbine by Ibrahim and Nienow (1996).

Stagnant particles are observed in this work for the MW and LW, either at the tank centre at annular region where the main flow meets with the inward flows. The formation of the reversible radial flow at the corners is similar to as reported by Kumaresan and Joshi (2006) in a 6 bladed pitched blade turbine. The authors explained that the presence of reversible radial flow is unfavorable in solid liquid mixing as it can cause stagnant particles to form at the tank base.

4.6.2 Flow pattern of 3P (d80)

3P (d80) is an axial impeller. This impeller is able to keep the downward axial flow all the way to the tank base up to *C*/*D* = 0.75, unlike the 4PBT for which secondary recirculation loop took over the flow on the base at *C*/*D*=0.75. The reversible radial-flow below the impeller is formed starting from the clearance 0.50, however the ones in the 4PBT appears to be more axial. Sometimes, an inward flow is formed under the baffles, where particles occasionally fall off from the main flow and drop back to the base. This additional inward flow was not present at all times, however it was observed to form more frequently with the 3P (d80) than the 4PBT. Tracer particles movements are observed to be weakened when the flow from different direction meets.

At the highest clearance of *C*/*D* = 1.0, the discharge stream does not have sufficient momentum to reach the tank base and a double-eight flow was formed. Tracer particles tend to fall off from the secondary flow to the base when the flow is weak until a stronger gush of fluid picks up the fallen particles back into the flow stream. Tracer particles were often found accumulating at the tank centre and a weak flow from the secondary inward flow was observed to weakly draw the top layer of tracer particles towards the impeller. Figure 4.6 shows that the last point to suspend PMMA in this configuration with high clearance is always at the tank centre. ε_{js} appeared to have a sudden peak at this clearance with the presence of the radial-like flow , especially when suspending the LW particles.

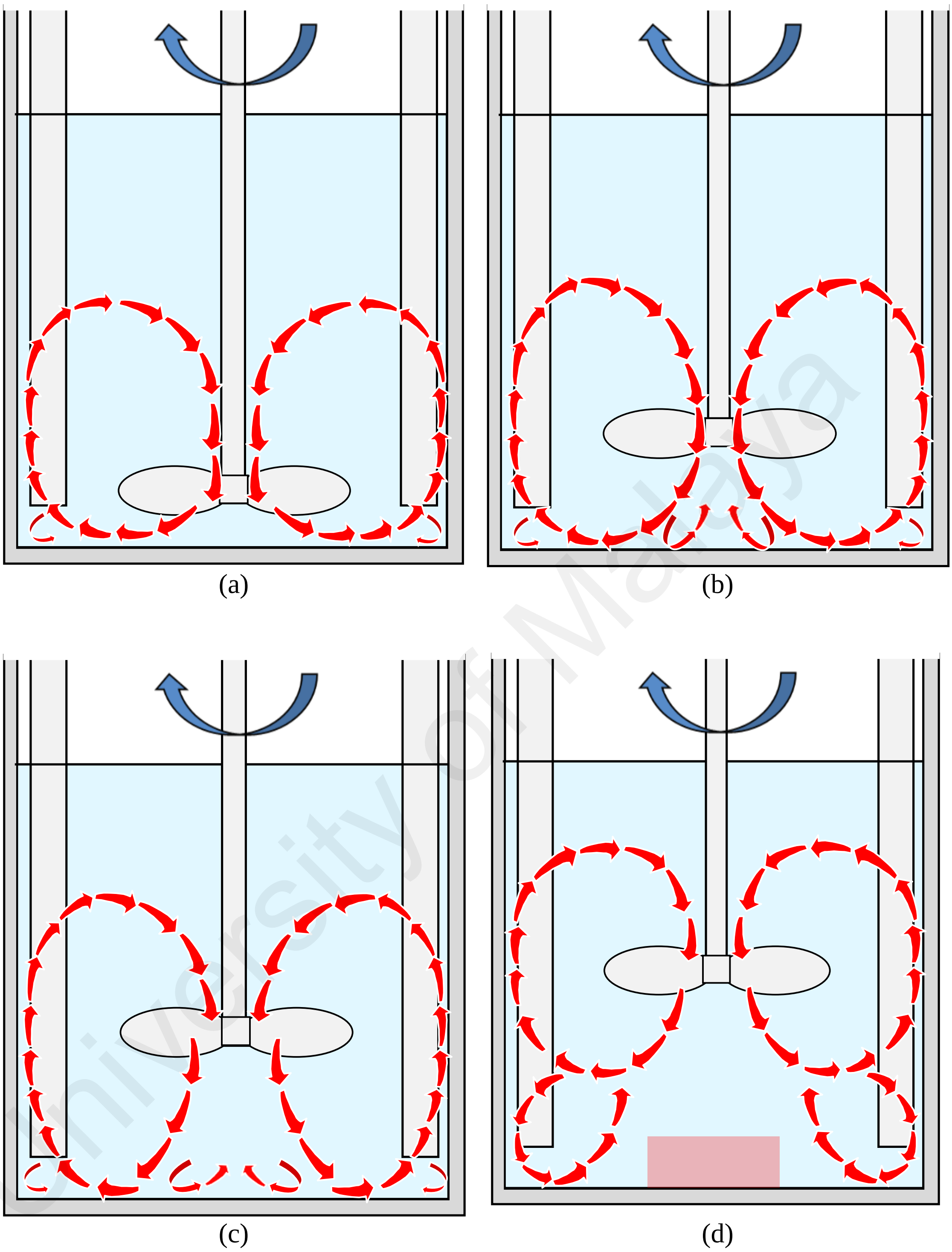

Figure 4.8: Flow pattern in 3P (d80) (a) *C/D* = 0.25; (b) *C/D* = 0.50; (c) *C/D* = 0.75; (d) *C/D* = 1.00

4.6.3 Flow pattern of HR100

HR100 is an axial impeller. Unlike the 4PBT, the discharge stream is fully axial, and the discharge is very powerful that even at the highest clearance of C/D=1.0 the axial flow reached the tank base. Figure 4.4 illustrates the main flow observed, however the tracer particles are pumped and drawn down from above $H/2$. The strong axial flow eliminates the accumulation of solid particles at centre of the base. While the central region was seen to be the weakest point for 3P (d80) and 4PBT of similar D/T, this is apparently not so for HR100, since its last point is often at the annular region or the side. The only time the last point of suspension occurred at the tank centre was when suspending 40wt% of LW particles at clearance 1.00. The inward recirculation flows at the corners are stronger at lower clearances compared to C/D of 0.75 and 1.00. Tracer particles at tank centre were observed to fall back to the base as they lost their momentum, but they were quickly swept away by the main flow. Similar to the observation at the tank base, solid particles at the tank centre are often observed to be pumped outward and easily lifted from the tank base.

Stagnant particles are observed at the tank centre or in an annular ring, only in MW and LW particles, where reversible flow observed at the corners and tank centre collides with the main flow.

N_{js} and ε_{js} using a HR100 is least affected by clearances among the impellers studied as the strong axial discharge has good consistency throughout all studied clearances. The discharge stream is only observed to be weakened at higher clearances, where a higher increase in impeller speed is needed to suspend particles at high concentration.

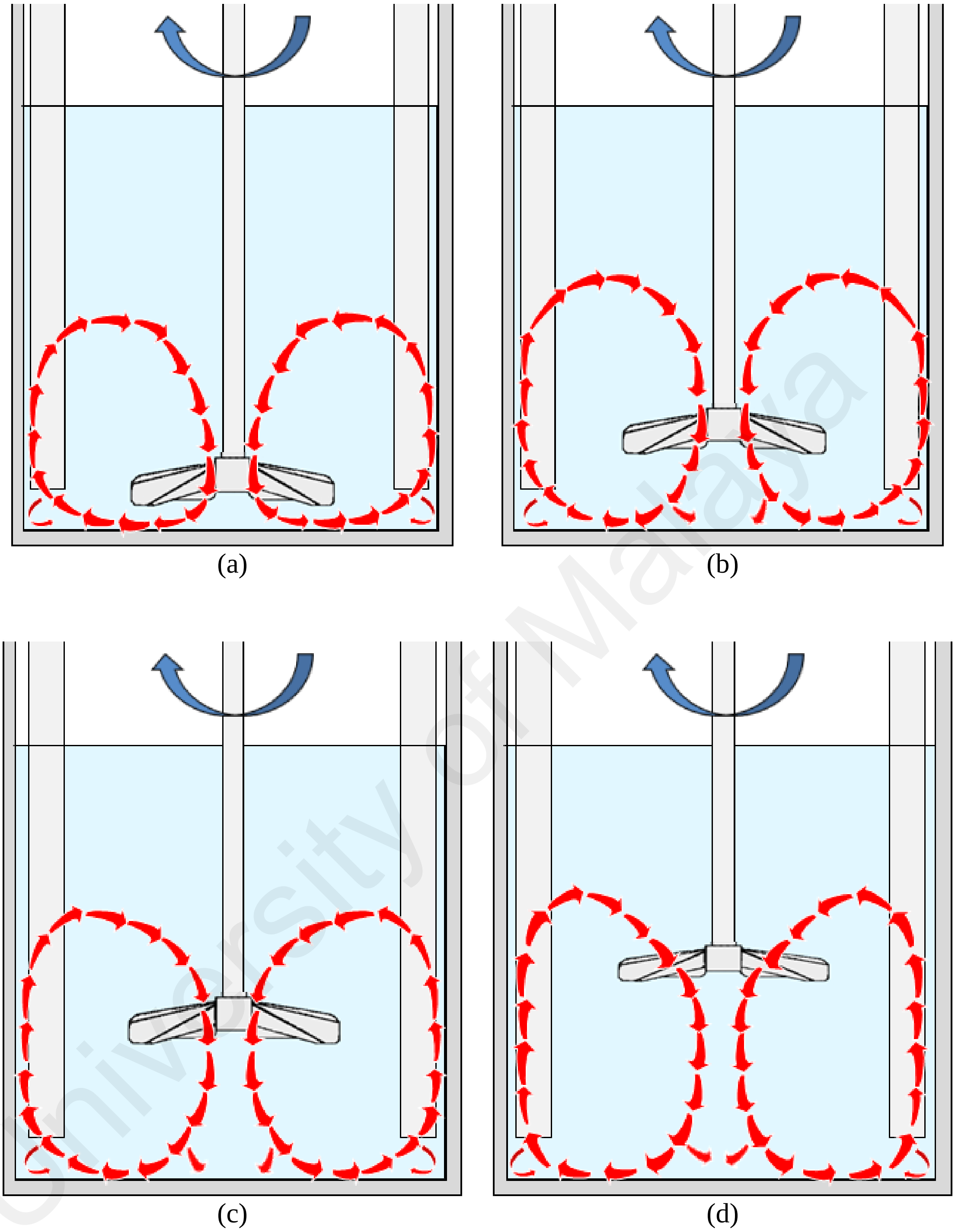

Figure 4.9: Flow pattern in HR100 (a) C/D = 0.25; (b) C/D = 0.50; (c) C/D = 0.75; (d) C/D = 1.00

4.6.4 Flow Pattern of HS604

HS604 is a novel impeller designed to operate at low impeller speed. Placing the impeller at low clearance generates radial flow along the tank base and a large circulation up to the top of the tank. The N_{js} using HS604 is low even in high concentrations, but the mixing is homogenous up to the full liquid height.

Figure 4.6 shows that solid particles at between centre and sides are easily lifted, solid particles at tank centre are as though trapped beneath the hub, while particles at the sides are last to be lifted. The amount of solid particles remaining unsuspended at tank centre is very little compared to the other impellers. Slight increase of impeller speed and the trapped solid particles at the tank centre are released and drifted with the main flow. Figure 4.10 shows that secondary flow is absent with the HS604 and this explains why the solid particles is last to be suspended at the sides for all experiments. However the flow does not easily reaches to the circumference of the tank, hence tracer particles are often last to be suspended at the sides as shown in Figure 4.6. Generally, HS604 operates at a relatively low impeller speed, even to suspend LW particles. The strong discharge flow hits the base, easily lifts the solid particles at low clearance.

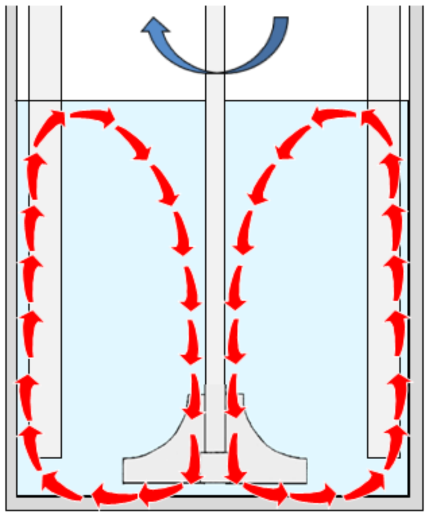

Figure 4.10: Flow pattern in HS604

As lightweight particles are easily suspended, the presence of the secondary recirculation loop helps to suspend the particles, especially the SW particles. However the presence of the secondary flow results in the presence of stagnant particles when suspending the MW and LW particles. These particles of larger d_p could be trapped by the two flows of different directions and remained at the tank base as stagnant particles. The regions of stagnation are absent in smaller particles of sizes d_p 18.6 µm and 27±4 µm (Results not shown). Impeller flow pattern varies with impeller geometries and it determines how particles are suspended from the tank base. Generally the discharge stream is weakened at higher clearances where a higher increase in impeller speed is required to suspend the particles at high concentration. This phenomena is more pronounced in the 4PBT impeller, which produces mixed-flow. At C/D of 0.75 and 1.00, the radial discharge by the 4PBT is clearly inefficient to pick up the settling solid particles. The full double loop discharge is only observed in C/D=1.00 for the 3P (d80), where similar increase in ε_{js} is also observed in the C/D=0.75 for the 4PBT. It is shown that the flow pattern of HR100 is least affected by the change in impeller clearance, which explains the consistent ε_{js} throughout all clearances. HS604 produces a strong radial flow, and the particles are well suspended up to the top of the tank. In a nutshell, axial flow pattern is more effective than radial flow pattern to suspend the lightweight fine particles.

4.7 Zwietering *S* value

In this work, the just-suspension speed was determined visually and used in Zwietering's equation to calculate the values of S under different operating conditions. Naturally the trends observed for S reflect the trends for N_{js}. Availability of S values for the conditions studied would enable future prediction of the N_{js} in the instance that some parameters other than geometry are changed.

Accurate prediction of the just suspension speed using Zwietering's correlation is dependent on the values used for the geometric parameter, S. Other parameters in Zwietering's correlation are properties of liquid and particles, are more readily available than the S values. Zwietering had illustrated that S is a function of impeller/tank geometry. Ideally S should only be a function of the geometry, but Machado et al., (2011), Ibrahim and Nienow, (1996) and Ibrahim et al., (2012) demonstrated with bronze and glass beads and activated carbon particles that S is also dependent on particle type and concentration.

In this study, with the range of conditions used, including different sizes and concentration for the same type of particles, the effects of particle size, d_p and concentration, X were observed. The range for which Zwietering's equation will give predictable values of N_{js} is determined for the conditions studied in this work.

The experimental *S* values are as shown in Table 4.1 and 4.2, and these values are plotted in Figure 4.11 for *S* versus impeller clearance. Figure 4.11(a)-(d) illustrates how *S* responds to change in clearance, concentration and particle sizes for 4PBT, 3P (d80), 3P (d60), and HR100. As already reported by Zwietering, the *S* values are shown here to be sensitive to change in clearance, especially for the 4PBT and 3P (d80), with a few exception between *C*/*D*=0.25 to 0.5. Interestingly, *S* values changes with clearance is subject to the particle size used. *S* linearly increases with clearance for the SW particles, while with LW particles the *S* values are very similar at the *C*/*D* 0.25 and 0.50. With regard to particle size, the LW particles show a more significant increase of *S* at increasing concentration, compared to the other particles.

For HR100, *S* linearly increases from clearance 0.25 to 0.75, *S* at *C*/*D* = 1.00 and 0.75 is similar. This applies for all three particle sizes. *S* is similar for all concentrations when suspending MW, and *S* is lower in MW particles than SW and LW particles for all impeller geometries. Increasing concentration leads to higher *S* for SW and LW particles throughout the studied clearances, with a similar gradient.

Ayranci and Kresta (2011) showed that for an axial impeller A310, the relationship between *S* and clearance can be expressed in linear form. HR100 shows near-linear relationship with the effect of clearance. In the same study by Ayranci and Kresta (2011), *S* value in a mixed flow impeller PBT, could best be described with a polynomial curve. In earlier studies, Chudacek (1986) also reported that the effect of clearance on *S* values cannot be expressed in power law form.

For HR100, the S values between adjacent clearances (i.e. 0.25D and 0.50D, 0.50D and 0.75D, 0.75$D$and 1.00D) have less than 10% difference but when comparing the S values between clearances further apart (e.g. C/D = 0.50 and 1.00). Ayranci and Kresta (2011) reported that for $C/T< 0.25$ ($\approx C/D \leq 0.50$) the effect of change in clearance is small but higher clearances where secondary loop is present, the effect of clearance will be significant. For 4PBT, the secondary inward flow starts to present at $C/D \geq 0.75$, however for all studied particles the difference of S values are insignificant between clearance 0.50 and 0.75.

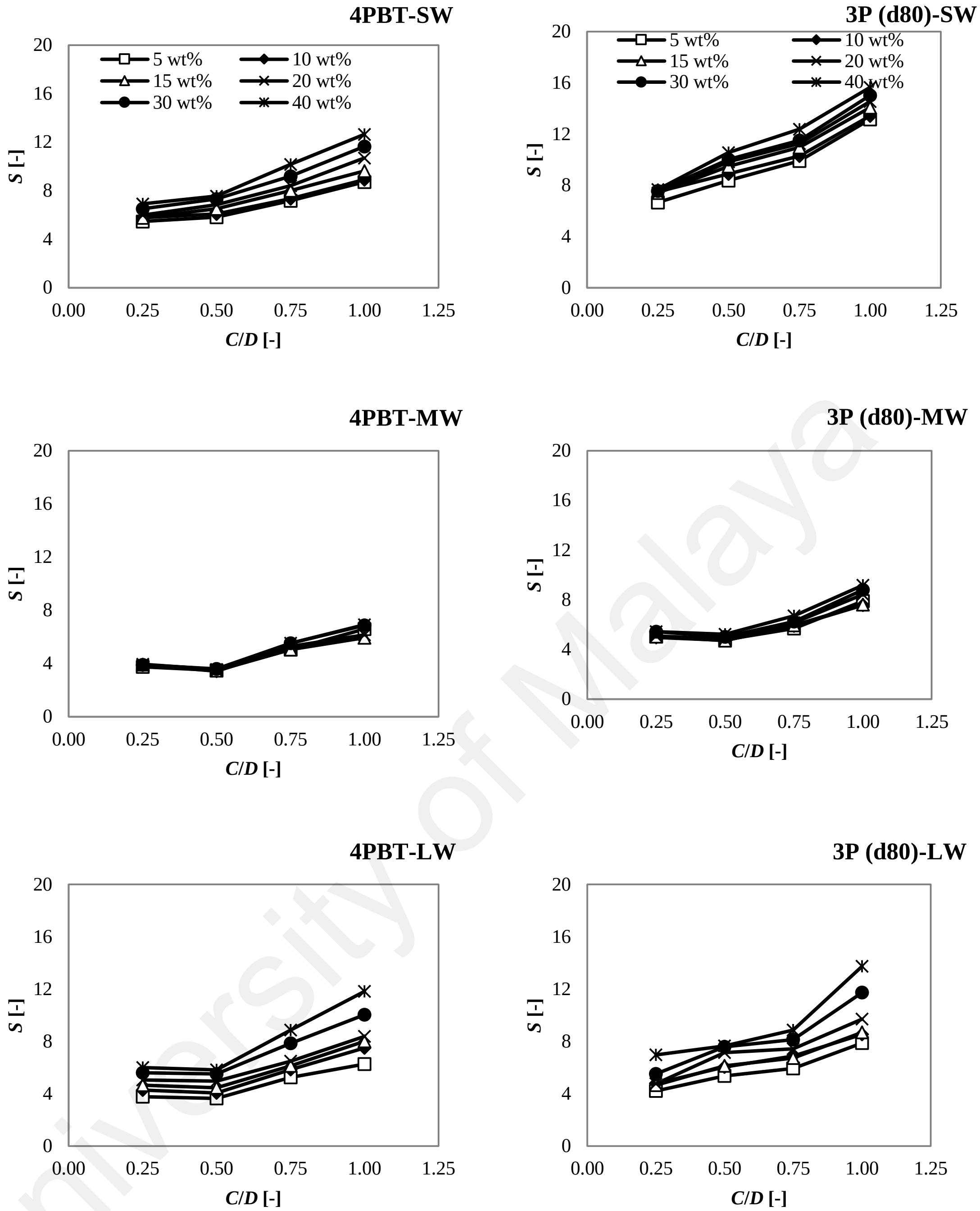

(a) (b)

Figure 4.11: Effect of clearance on *S* values for (a) 4PBT; (b) 3P (d80)

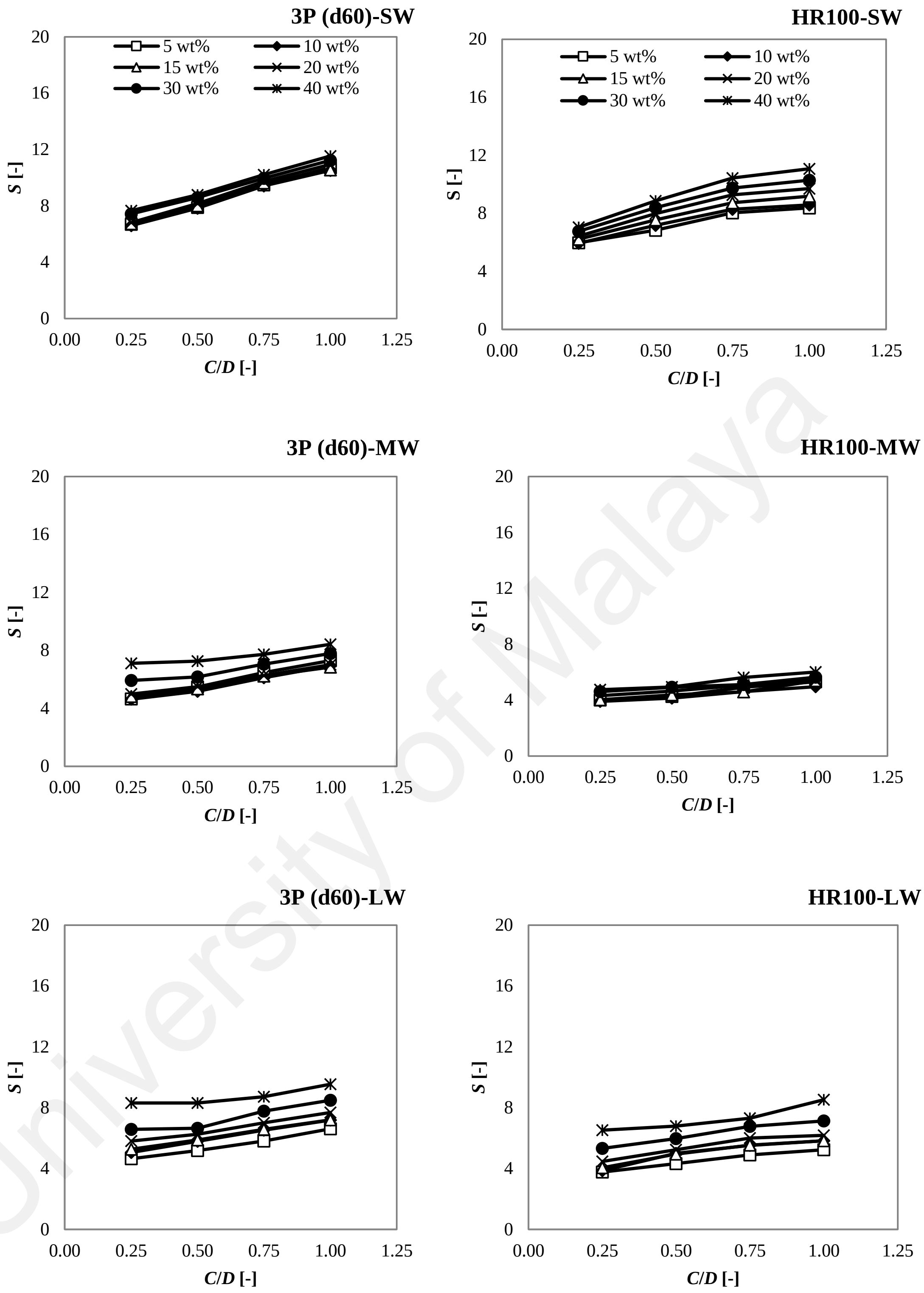

(c) (d)

Figure 4.11, continued: (c) 3P (d60); (d) HR100

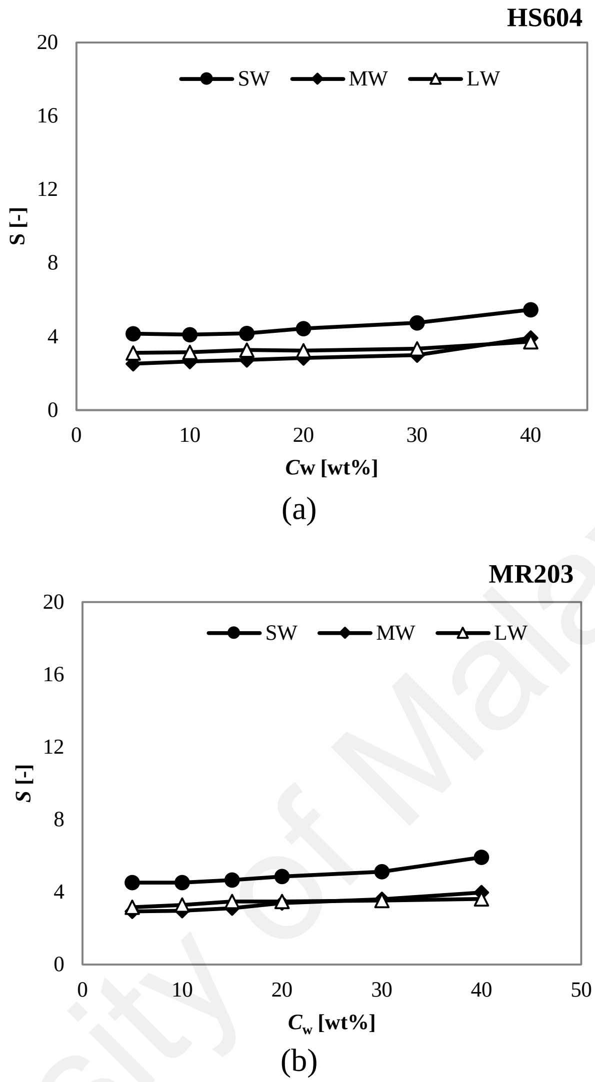

Figure 4.12: Effect of concentration on *S* values for (a) HS604; (b) MR203

Table 4.1: Experimental *S* values

		4PBT			3P (d80)			3P (d60)			HR100		
C/D	wt%	SW	MW	LW	SW	MW	LW	SW	MW	LW	SW	MW	LW
0.25	5	5.47	3.75	3.76	6.66	5.04	4.22	6.69	4.65	4.64	5.98	4.01	3.76
	10	5.78	3.90	4.27	7.49	4.96	4.79	6.60	4.62	5.06	5.93	3.90	3.85
	15	5.78	3.92	4.65	7.41	5.04	4.65	6.73	4.82	5.26	6.22	4.03	4.05
	20	5.99	3.88	5.05	7.42	5.07	4.76	6.82	4.98	5.81	6.42	4.32	4.47
	30	6.50	3.89	5.60	7.58	5.42	5.51	7.42	5.93	6.58	6.77	4.61	5.33
	40	6.91	3.94	6.00	7.69	5.42	6.96	7.66	7.10	8.31	7.04	4.73	6.52
0.5	5	5.81	3.49	3.65	8.37	4.78	5.36	7.89	5.46	5.18	6.83	4.26	4.33
	10	6.09	3.42	4.06	8.90	4.72	6.04	7.82	5.18	5.79	7.18	4.13	5.00
	15	6.52	3.47	4.45	9.48	4.70	6.13	8.00	5.35	5.88	7.55	4.37	4.94
	20	6.85	3.45	4.95	9.84	4.86	7.14	8.16	5.49	6.26	7.99	4.64	5.24
	30	7.31	3.58	5.51	10.02	5.02	7.59	8.59	6.17	6.65	8.39	4.91	5.96
	40	7.56	3.55	5.83	10.56	5.23	7.66	8.78	7.26	8.31	8.87	4.93	6.79
0.75	5	7.18	5.04	5.24	9.91	5.68	5.93	9.50	6.48	5.80	8.03	4.91	4.90
	10	7.34	5.19	5.83	10.30	5.90	6.88	9.41	6.10	6.53	8.27	4.60	5.52
	15	8.00	5.04	6.13	10.96	5.94	6.72	9.63	6.23	6.58	8.74	4.59	5.53
	20	8.42	5.29	6.47	11.27	6.15	7.43	9.72	6.25	7.01	9.27	5.07	6.00
	30	9.20	5.53	7.86	11.50	6.24	8.13	9.96	7.05	7.78	9.75	5.12	6.77
	40	10.17	5.52	8.87	10.17	6.70	8.87	10.21	7.72	8.72	10.43	5.62	7.31
1.00	5	8.71	6.59	6.27	7.49	7.88	7.87	6.60	7.28	6.61	5.93	5.30	5.24
	10	8.90	6.14	7.50	13.43	7.56	8.54	10.51	6.93	7.18	8.59	4.96	5.83
	15	9.63	5.94	8.01	14.07	7.62	8.70	10.55	6.84	7.20	9.18	5.38	5.83
	20	10.70	6.15	8.38	14.55	8.42	9.71	10.95	7.01	7.68	9.70	5.39	6.19
	30	11.64	6.86	10.02	15.02	8.80	11.74	11.23	7.77	8.49	10.29	5.63	7.13
	40	12.65	6.90	11.83	15.65	9.17	13.75	11.54	8.42	9.54	11.08	6.01	8.53

Table 4.2: Experimental *S* values for HS604 and MR203

	HS604			MR203		
wt%	SW	MW	LW	SW	MW	LW
5	4.16	2.52	3.11	4.52	2.93	3.16
10	4.10	2.64	3.14	4.52	2.98	3.28
15	4.18	2.73	3.27	4.67	3.10	3.49
20	4.44	2.84	3.24	4.85	3.40	3.48
30	4.74	2.99	3.34	5.12	3.61	3.53
40	5.46	3.93	3.73	5.91	3.98	3.62

Experimental S values are compared with literature values at similar clearance (Ibrahim & Nienow, 1996); Ayranci & Kresta, 2011) using different but similar impeller geometries in Figures 4.13 and 4.14. Figures 4.13 (a) and 4.13 (b) show the S values of 3 bladed-impellers with $D/T \approx 1/2$ and $D/T \approx 1/3$, respectively. The S values were taken with different types of solid particles, hence having different densities. In addition, the tank size, particle size and concentrations also differ from one work to another. Nevertheless, it is still interesting to see how these S values fall within a range shown in the plots. For example, data points of HR100 are from the 5wt% of this work while data for A310 and HE-3 from Ibrahim and Nienow, (1996), were done at 0.5wt%. Generally, SW particles have higher S values of >5.0, falling in the same level with the particles of much higher density, such as BLGB and bronze. S values of HR100 in MW and LW would fall in a lower range of <4.0, quite distant from those in SW.

Figure 4.14 shows data for 4PBT of $T/2$ in this study and also $T/3$ (Ayranci & Kresta, 2011). The literature S values by Ayranci and Kresta (2011) is always higher than the values obtained in this study; and this could possibly attributed to the density of particles. Small glass beads and large glass beads (SG and LG) with 4PBT have S which are very similar (<10% difference), just as MW and LW in the HR100, 3P (d80) and 4PBT. S in SW could have >60% difference from the MW and LW sizes.

Trend line on the S plot appears to have a gradient similar to those in N_{js} and ε_{js} plots, just as reported in the study by Ayranci and Kresta (2011). Impeller clearance would give a similar effect on the S values, as it is to the N_{js} and ε_{js}. Figures 4.13 and 4.14 show that S for small glass beads (SG) is lower than SW particles.

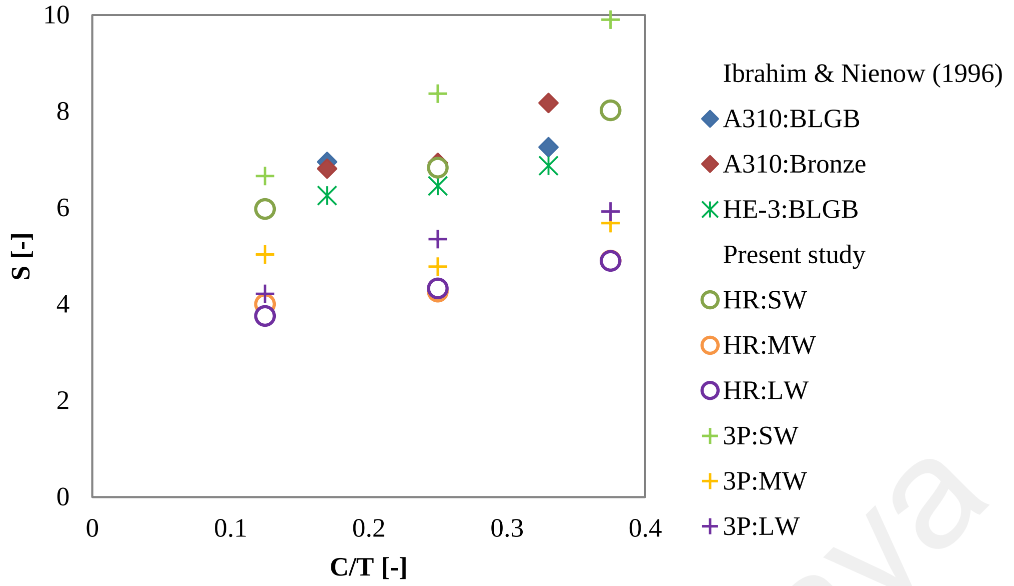

(a)

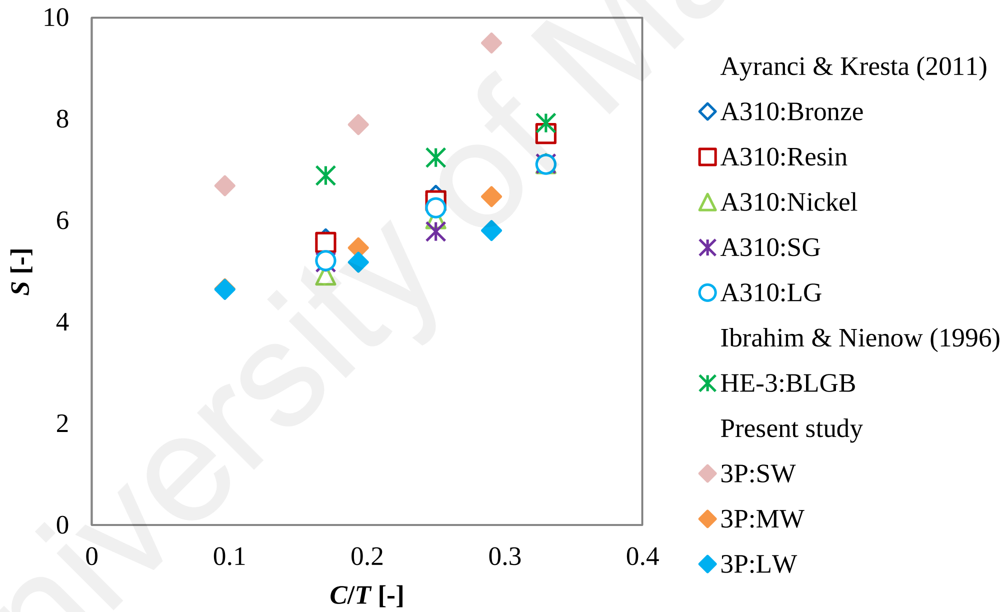

(b)

Figure 4.13: Experimental and literature S values in 3-bladed impellers (a) $T/2$; (b) $T/3$

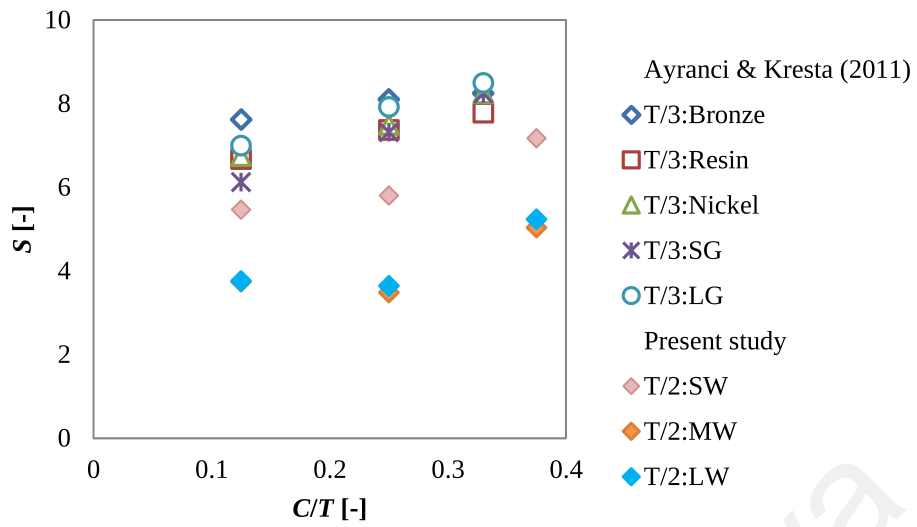

Figure 4.14: Experimental and literature *S* values of 4PBT *T*/3 and *T*/2

It is shown in this work that factors other than impeller geometries, such as concentration and particle size, are not well defined Equation (1). Zwietering (1958) only used solids concentration up to 20% and as this work uses concentration up to 40wt%, the errors in the *S* values calculation exceeds 10%. However, it is noteworthy that the *S* values in HS604 and MR203 are less susceptible to the change in concentration compared to all other impellers, as error >10% are only present at a single concentration of 40wt%.

CHAPTER 5

CONCLUSIONS AND RECOMMENDATIONS

5.1 Conclusions

Solids suspension has been studied using PMMA solids of different sizes and concentrations in a fully-baffled flat-based cylindrical stirred tank of 15.5cm diameter. Suspension with different geometries were achieved through the use of novel SATAKE designs in comparison to standard pitched-blade and propeller types D/T=0.52 for all impellers, and 0.39 for one propeller (3P (d60)). Power measurement at the minimum speed for just-suspension, N_{js}, enabled the efficiency of the impellers to be assessed. In addition, this work also looked at the effect of particle size and concentration, and impeller clearance on particles distribution on the tank base in relation to the impeller flow pattern, and how this relates to N_{js}. The findings can be summarized as follows:-

- Flow patterns generated by the impellers directly govern particle distribution and movements on the tank base. Knowing the impeller flow pattern can provide a means of predicting how the particles will be suspended from the base and the relative power requirement.
- In this work where lightweight fine particles are studied, axial flow is found to be more effective in suspending the particles than radial flow. The axial flow of the 4PBT and 3P (d80) were dampened as the clearance increased, and recirculation loops were clearly observed in the lower region beginning from C/D of 0.75 and 1.0, respectively. This created a radial-like effect in the lower region with flow moving inwards on the base. On the other hand the HR100 maintained the axial motion throughout the range of clearances. These effects were reflected by the particles distribution on the base

- Increase in clearance has the effect of increasing the N_{js} and ε_{js}, with the exception of the 4PBT in going from *C*/*D*=0.25 to 0.5. The increase in speed and power demand was most significant at the higher clearances for the standard impellers, where the flow pattern change from totally axial to pseudo-radial was noted. By comparison, the HR100 and 3P (d60) were found to be least affected by the change in clearance and for HR100 at least, this is attributed to the fact that the flow remained axial throughout the range of clearance.
- The change in clearance was found to have least effect on ε_{js} when suspending MW particles for the 4PBT and 3P (d80).
- Interestingly the ε_{js} in using SW are always higher than MW experiments. It could be that the SW size is beyond a certain critical size related to the minimum power as reported by Wang et al. (2012). However, for the radial HS604 impeller only a small variation is seen in ε_{js} for the different d_p used. Axial flow impellers are found generally more energy efficient for suspending the solid particles than radial impellers. Overall the novel HR100 and HS604 were found to be the most energy efficient in terms of suspending particles, but the 3P (d60) performance matches these novel impellers very closely. In addition, particles were observed to be easily suspended with the large MR203 impellers at extra-low clearance, but required much higher power input compared to other impellers.
- *S* values do not change significantly with increase in clearance by 0.25*D*. The difference only becomes significant when the change in clearance is up to 0.50 *D* (≈0.25*T*). As mentioned above, increase in clearance for 4PBT and 3P (d80) may produce secondary inward flow beneath the impeller, while the HR100 has a consistent flow pattern throughout all clearances, and this is also reflected in the *S* values.

- Calculated *S* values from the Zwietering's correlation could have errors >10% in slurries of different concentrations. The occurrence is most often found in 40wt% for the HS604 and MR203 impellers, and in the higher concentrations of 20wt% and above of LW particles.

5.2 Recommendation

For solids suspension in stirred tank, the impeller flow pattern is a good indication of how particles are lifted from the tank base, and in turn, the power required to achieve solids suspension. Investigation of the mean velocity field at the tank base could be useful to investigate the effect of the flow induced by impellers on particles movements at tank base, and relating its effect on the ε_{js} for the experimental conditions. The use of solids of different properties could also provide more insight on the mechanism for suspension.

REFERENCES

Armenante, P. M., & Nagamine, E. U. (1998). Effect of low off-bottom impeller clearance on the minimum agitation speed for complete suspension of solids in stirred tanks. *Chemical Engineering Science, 53*(9), 1757-1775.

Aubin, J., Le Sauze, N., Bertrand, J., Fletcher, D. F., & Xuereb, C. (2004). PIV measurements of flow in an aerated tank stirred by a down-and an up-pumping axial flow impeller. *Experimental thermal and fluid science, 28*(5), 447-456.

Ayranci, I., & Kresta, S. M. (2011). Design rules for suspending concentrated mixtures of solids in stirred tanks. *Chemical Engineering Research and Design, 89*(10), 1961-1971. .

Ayranci, I., Machado, M. B., Madej, A. M., Derksen, J. J., Nobes, D. S., & Kresta, S. M. (2012). Effect of geometry on the mechanisms for off-bottom solids suspension in a stirred tank. *Chemical Engineering Science, 79*(10), 163–176.

Ayranci, I., Ng, T., Etchells Iii, A. W., & Kresta, S. M. (2013). Prediction of just suspended speed for mixed slurries at high solids loadings. *Chemical Engineering Research and Design, 91*(2), 227-233.

Aziz, A., Ibrahim, S., & Parthasarathy, R. (1999). *Determination of just-suspension speed for Rushton turbine using tank bottom pressure measurements.* Paper presented at the Institution of Chemical Engineers Symposium Series.

Baldi, G., Conti, R., & Alaria, E. (1978). Complete suspension of particles in mechanically agitated vessels. *Chemical Engineering Science, 33*(1), 21-25.

Bates, R. L., Fondy, P. L., & Corpstein, R. R. (1963). Examination of some geometric parameters of impeller power. *Industrial & Engineering Chemistry Process Design and Development, 2*(4), 310-314.

Bubbico, R., Cave, S. D., & Mazzarotta, B. (1998). Agitation power for solid-liquid suspensions containing large particles. *The Canadian Journal of Chemical Engineering, 76*(3), 428-432.

Bujalski, W., Takenaka, K., Paoleni, S., Jahoda, M., Paglianti, A., Takahashi, K., . . . Etchells, A. (1999). Suspension and liquid homogenization in high solids concentration stirred chemical reactors. *Chemical Engineering Research and Design, 77*(3), 241-247.

Chapman, C. M., Nienow, A. W., Cooke, M., & Middleton, J. (1983). Particle-gas-liquid mixing in stirred vessels. I: Particle-liquid mixing. *Chemical engineering research and design, 61*(2), 71-81.

Chapple, D., Kresta, S. M., Wall, A., & Afacan, A. (2002). The effect of impeller and tank geometry on power number for a pitched blade turbine. *Chemical Engineering Research and Design, 80*(4), 364-372.

Chudacek, M. W. (1985). Solids suspension behaviour in profiled bottom and flat bottom mixing tanks. *Chemical engineering science, 40*(3), 385-392.

Chudacek, M. W. (1986). Relationships between solids suspension criteria, mechanism of suspension, tank geometry, and scale-up parameters in stirred tanks. *Industrial & engineering chemistry fundamentals, 25*(3), 391-401.

Gray, D. J. (1987). Impeller clearance effect on off bottom particle suspension in agitated vessels. *Chemical Engineering Communications, 61*(1-6), 151-158.

Hicks, M. T., Myers, K. J., & Bakker, A. (1997). Cloud height in solids suspension agitation. *Chemical Engineering Communications, 160*(1), 137-155.

Hosseini, S., Patel, D., Ein-Mozaffari, F., & Mehrvar, M. (2010). Study of solid–liquid mixing in agitated tanks through electrical resistance tomography. *Chemical Engineering Science, 65*(4), 1374-1384.

Ibrahim, S., Jasnin, S., Wong, S., & Baker, I. (2012). Zwietering's Equation for the Suspension of Porous Particles and the Use of Curved Blade Impellers. *International Journal of Chemical Engineering, 2012*.

Ibrahim, S., & Nienow, A. W. (1995). Power curves and flow patterns for a range of impellers in Newtonian fluids: 40< Re< $5x10^5$. *Chemical engineering research & design, 73*(5), 485-491.

Ibrahim, S., & Nienow, A. W. (1996). Particle suspension in the turbulent regime: the effect of impeller type and impeller/vessel configuration. *Chemical engineering research & design, 74*(6), 679-688.

Ibrahim, S., & Nienow, A. W. (1999). Comparing impeller performance for solid-suspension in the transitional flow regime with Newtonian fluids. *Chemical Engineering Research and Design, 77*(8), 721-727.

Ibrahim, S., & Nienow, A. W. (2004). Suspension of microcarriers for cell culture with axial flow impellers. *Chemical Engineering Research and Design, 82*(9), 1082-1088.

Jirout, T., & Rieger, F. (2011). Impeller design for mixing of suspensions. *Chemical Engineering Research and Design, 89*(7), 1144-1151.

Kasat, G. R., & Pandit, A. B. (2005). Review on Mixing Characteristics in Solid-Liquid and Solid-Liquid-Gas Reactor Vessels. *The Canadian Journal of Chemical Engineering, 83*(4), 618-643.

Kumaresan, T., & Joshi, J. B. (2006). Effect of impeller design on the flow pattern and mixing in stirred tanks. *Chemical engineering journal, 115*(3), 173-193.

Kuzmanić, N., & Ljubičić, B. (2001). Suspension of floating solids with up-pumping pitched blade impellers; mixing time and power characteristics. *Chemical Engineering Journal, 84*(3), 325-333.

Machado, M. B., Nunhez, J. R., Nobes, D., & Kresta, S. M. (2012). Impeller characterization and selection: Balancing efficient hydrodynamics with process mixing requirements. *AIChE Journal, 58*(8), 2573-2588.

Mavros, P. (2001). Flow visualization in stirred vessels: A review of experimental techniques. *Chemical Engineering Research and Design, 79*(2), 113-127.

Nienow, A. W. (1968). Suspension of solid particles in turbine agitated baffled vessels. *Chemical Engineering Science, 23*(12), 1453-1459.

Nienow, A. W., & Miles, D. (1978). The effect of impeller/tank, configurations on fluid-particle mass transfer. *The Chemical Engineering Journal, 15*(1), 13-24.

Nienow, AW. (1992) Suspension of solids in liquids. In N. Harnby, MF Edward & AW. Nienow (2nd ed.), *Mixing in the process industries* (pp. 364-393). London: Butterworth Heinemann.

Ochieng, A., & Lewis, A. E. (2006). Nickel solids concentration distribution in a stirred tank. *Minerals engineering, 19*(2), 180-189.

Paul, EL., Atiemo-Obeng, V.A. & Kresta, SM. (2004). .In *Handbook of industrial mixing: Science and practice* (pp. 543-584). New Jersey, NJ: Wiley Interscience.

Raghava Rao, K., Rewatkar, V., & Joshi, J. (1988). Critical impeller speed for solid suspension in mechanically agitated contactors. *AIChE journal, 34*(8), 1332-1340.

Sharma, R. N., & Shaikh, A. A. (2003). Solids suspension in stirred tanks with pitched blade turbines. *Chemical engineering science, 58*(10), 2123-2140.

Stevenson, R., Harrison, S. T., Mantle, M. D., Sederman, A. J., Moraczewski, T. L., & Johns, M. L. (2010). Analysis of partial suspension in stirred mixing cells using both MRI and ERT. *Chemical Engineering Science, 65*(4), 1385-1393.

Wang, J. (2010). *Suspension of high concentration slurry in agitated vessels* (Master's thesis). Retrieved from http://researchbank.rmit.edu.au/eserv/rmit:6402 /Wang.pdf

Wang, S., Boger, D. V., & Wu, J. (2012). Energy efficient solids suspension in an agitated vessel–water slurry. *Chemical Engineering Science, 74*, 233-243.

Wu, J., Graham, L. J., Nguyen, B., & Nabil Noui Mehidi, M. (2006). Energy efficiency study on axial flow impellers. *Chemical Engineering and Processing: Process Intensification, 45*(8), 625-632.

Wu, J., Graham, L., Wang, S., & Parthasarathy, R. (2010). Energy efficient slurry holding and transport. *Minerals Engineering, 23*(9), 705-712.

Wu, J., Zhu, Y. G., Bandopadhayay, P., Pullum, L., & Shepherd, I. (2000). Solids suspension with axial-flow impellers. *AIChE journal, 46*(3), 647-650.

Wu, J., Zhu, Y. G., & Pullum, L. (2002). Suspension of high concentration slurry. *AIChE journal, 48*(6), 1349-1352.

Zhou, Z., Scales, P. J., & Boger, D. V. (2001). Chemical and physical control of the rheology of concentrated metal oxide suspensions. *Chemical Engineering Science, 56*(9), 2901-2920.

Zwietering, T. N. (1958). Suspending of solid particles in liquid by agitators. *Chemical Engineering Science, 8*(3), 244-253.

List of publication and conference presentation

Wong, S. D., Ibrahim, S., Baker, I. F., Zamzam, Z., Sato, M.& Kato, Y. (2012). Suspension of High Concentration Fine Particles with Novel Axial and Radial Impellers. *Chemical Engineering Research and Design*. (Submitted)

Zamzam, Z., Kato, Y., Nemoto, T., Kanamori, H., Sato, M., Ibrahim, S., Wong, S. D., Baker, I. F. (2012). *A study of solid-liquid suspension in stirred tank using novel impeller geometries.* In the NORTH AMERICAN MIXING CONFERENCE 23,Mexico.

Ibrahim, S., Wong, S. D., Zamzam, Z., Kato, Y. & Sato, M. (2013). *Geometric effects on solids suspension characteristics for a range of particle size and concentation.* In ASIA CONFERENCE ON MIXING, China.

APPENDIX A

Table 1: Estimation of errors for solids mass calculation

C_w (wt%)	Weight of solid particle X(g)	Weight of water (g)	Apparent density (kgm^{-3})	A (kg)	B (kg)	% difference
0.05	147.942	2810.898	1015	2.959	2.969	0.329
0.10	299.379	2694.409	1030	2.994	3.012	0.623
0.15	454.435	2575.134	1045	3.030	3.056	0.883
0.20	613.244	2452.974	1060	3.066	3.100	1.108
0.30	942.672	2199.568	1090	3.142	3.188	1.454
0.40	1288.851	1933.276	1120	3.222	3.276	1.662

A: sum of weight of solid particles and water

B: weight calculated from apparent density

APPENDIX B

Table 2: ε_{js} values ($\times 10^{-1}$)

		4PBT			3P (d80)			3P (d60)			HR100		
C/D	wt%	SW	MW	LW	SW	MW	LW	SW	MW	LW	SW	MW	LW
0.25	5	0.23	0.17	0.26	0.21	0.19	0.17	0.13	0.09	0.43	0.19	0.14	0.16
	10	0.33	0.24	0.50	0.42	0.23	0.36	0.17	0.12	0.72	0.24	0.18	0.23
	15	0.41	0.29	0.76	0.42	0.29	0.34	0.20	0.18	0.96	0.35	0.22	0.32
	20	0.51	0.31	0.98	0.48	0.33	0.41	0.23	0.20	1.47	0.43	0.30	0.47
	30	0.75	0.35	1.61	0.62	0.47	0.73	0.33	0.39	2.69	0.59	0.42	0.87
	40	0.96	0.38	2.03	0.73	0.52	1.65	0.42	0.72	5.74	0.75	0.49	1.82
0.5	5	0.21	0.10	0.18	0.32	0.14	0.26	0.17	0.13	0.44	0.18	0.12	0.16
	10	0.34	0.14	0.31	0.48	0.17	0.51	0.20	0.15	0.83	0.30	0.13	0.33
	15	0.49	0.16	0.53	0.64	0.18	0.60	0.25	0.18	1.04	0.39	0.18	0.39
	20	0.59	0.18	0.82	0.80	0.24	1.05	0.33	0.21	1.44	0.51	0.24	0.50
	30	0.88	0.22	1.26	1.00	0.29	1.45	0.43	0.35	2.05	0.68	0.33	0.84
	40	1.08	0.24	1.59	1.32	0.39	1.70	0.52	0.63	4.65	0.91	0.36	1.38
0.75	5	0.43	0.37	0.57	0.45	0.20	0.30	0.26	0.19	0.55	0.28	0.15	0.21
	10	0.62	0.52	0.99	0.64	0.29	0.67	0.31	0.19	1.05	0.40	0.17	0.39
	15	0.95	0.56	1.41	0.91	0.35	0.72	0.42	0.26	1.35	0.55	0.19	0.47
	20	1.20	0.72	1.79	1.12	0.43	1.07	0.48	0.28	1.78	0.72	0.28	0.70
	30	1.83	0.92	3.80	1.45	0.54	1.69	0.59	0.51	3.12	0.98	0.35	1.16
	40	2.58	0.96	6.05	1.89	0.77	2.43	0.74	0.73	5.00	1.29	0.49	1.67
1.00	5	0.82	0.72	1.05	1.10	0.58	0.80	0.34	0.26	0.77	0.34	0.20	0.29
	10	1.17	0.88	2.35	1.56	0.68	1.37	0.42	0.28	1.37	0.47	0.22	0.52
	15	1.76	0.94	3.35	2.00	0.79	1.69	0.51	0.32	1.63	0.69	0.31	0.59
	20	2.66	1.14	4.24	2.52	1.20	2.42	0.59	0.42	2.21	0.89	0.36	0.81
	30	3.81	1.79	8.15	3.30	1.56	5.31	0.74	0.66	3.59	1.22	0.49	1.47
	40	5.17	1.89	14.00	4.05	2.02	9.58	0.87	0.92	6.18	1.64	0.67	2.71

Table 3: ε_{js} values ($\times 10^{-1}$) for HS604 and MR203

	HS604			MR203		
wt%	SW	MW	LW	SW	MW	LW
5	0.25	0.13	0.34	0.91	0.51	1.01
10	0.33	0.19	0.47	1.14	0.71	1.41
15	0.39	0.24	0.62	1.37	0.96	1.96
20	0.52	0.30	0.66	1.70	1.37	2.19
30	0.74	0.39	0.82	2.30	1.85	2.68
40	1.17	0.98	1.25	3.75	2.75	3.12

APPENDIX C

The effect of clearance on power consumption for impellers

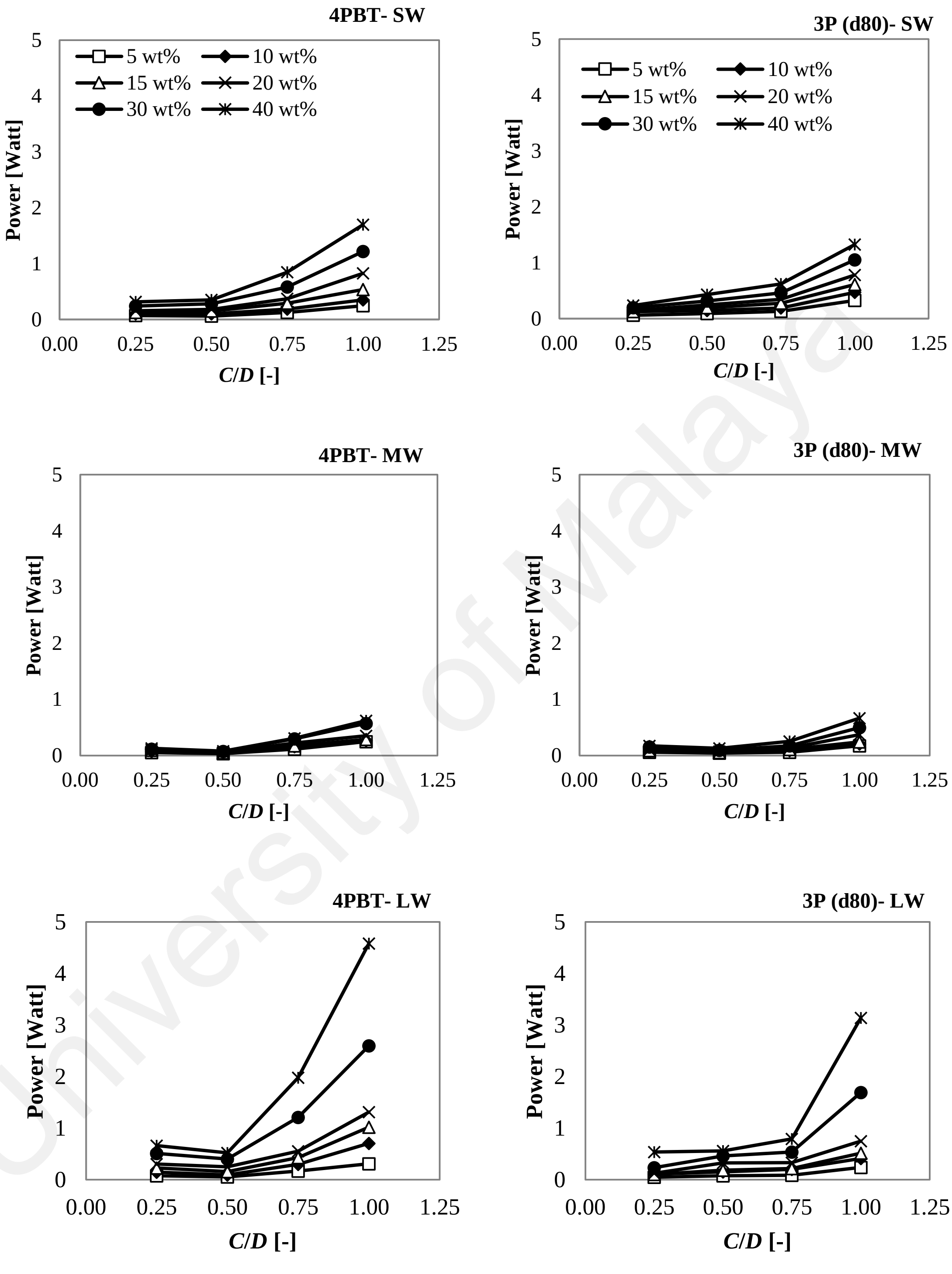

Figure 1: The effect of clearance on power for (a) 4PBT; (b) 3P (d80)

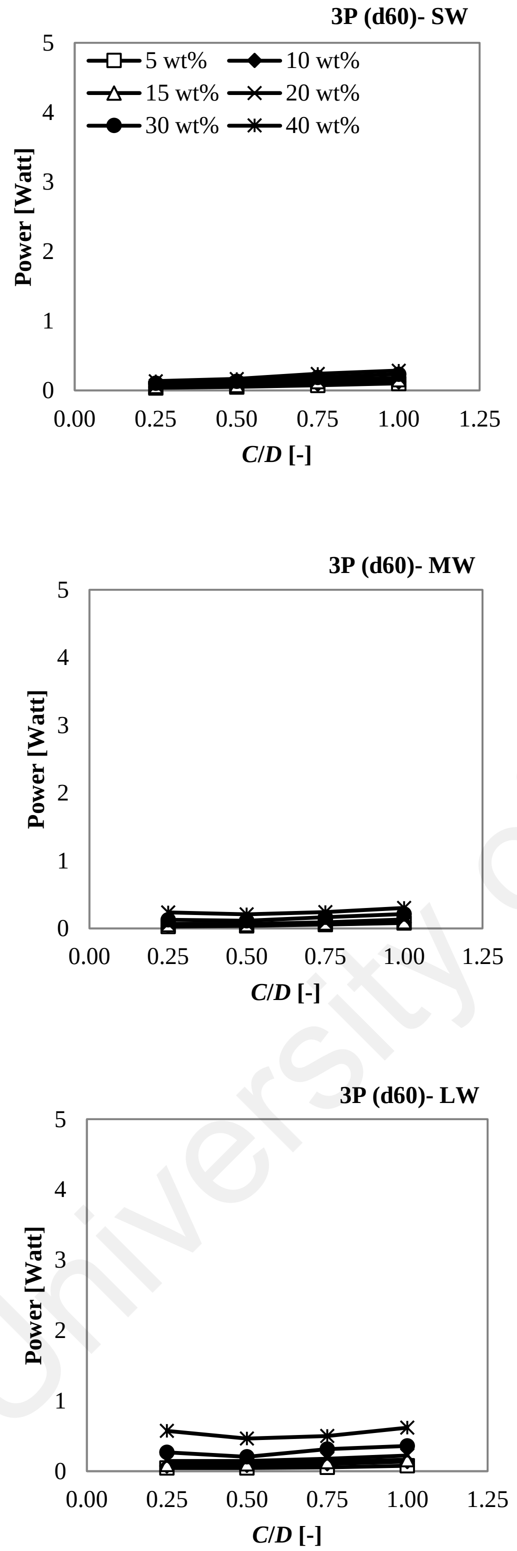

(c)

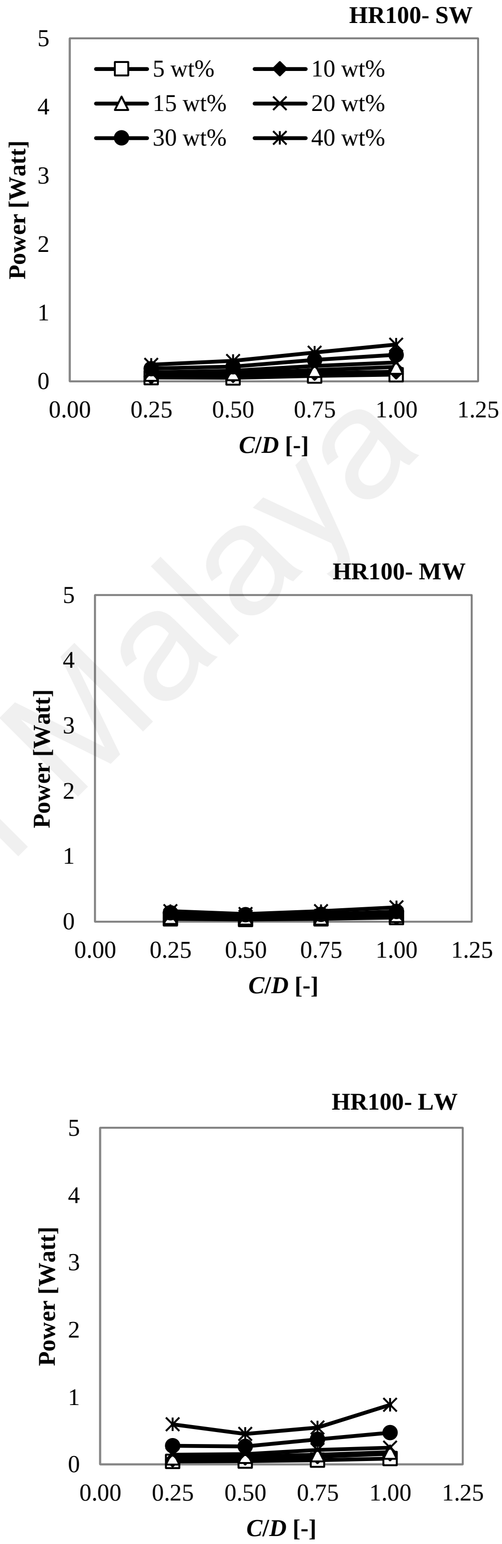

(d)

Figure 1, continued: The effect of clearance onspecific power for (c) 3P (d60); (d) HR100

APPENDIX D

The effect of concentration on power consumption for HS604 and MR203

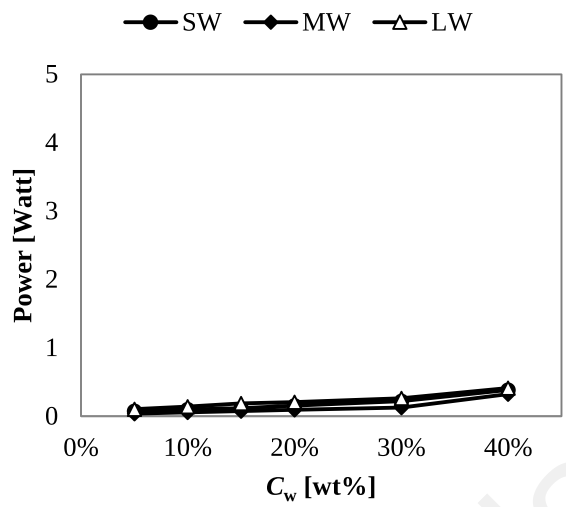

Figure 2: The effect of concentration on power in HS604

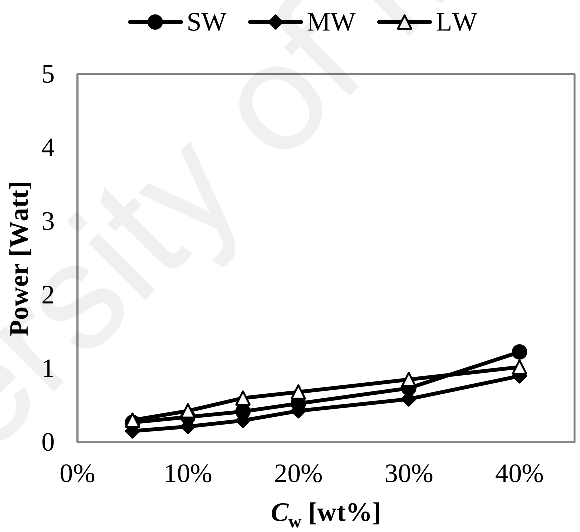

Figure 2: The effect of concentration on power in MR203

APPENDIX E

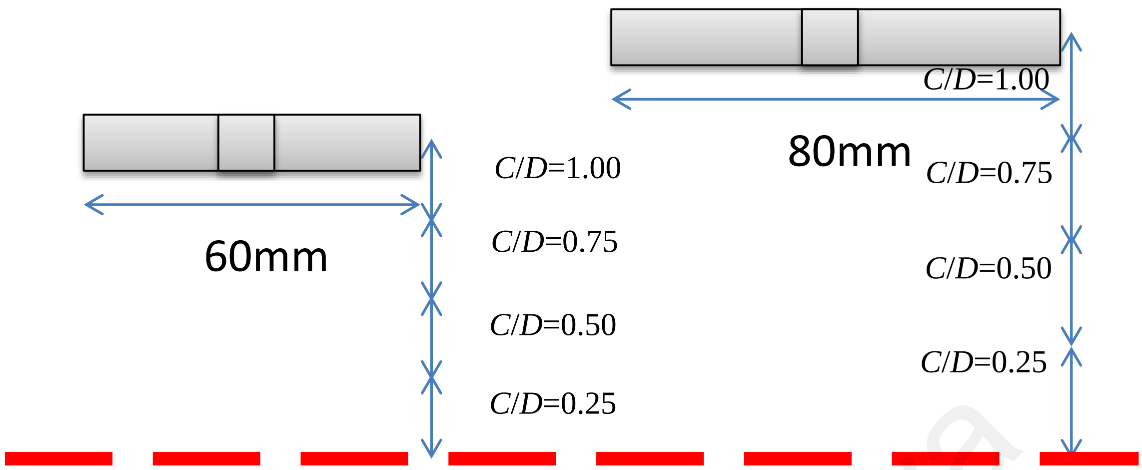

Figure 3: Impeller clearance measured from tank base